Plasmodium falciparum PhIL1 associated complex play an essential role in merozoite reorientation and invasion of host erythrocytes

Ekta Saini
International Centre for Genetic Engineering and Biotechnology https://orcid.org/0000-0001-5701-6108

Pradeep Kumar Sheokand
International Centre for Genetic Engineering and Biotechnology

Vaibhav Sharma
International Centre for Genetic Engineering and Biotechnology

Prakhar Agrawal
International Centre for Genetic Engineering and Biotechnology

Inderjeet Kaur
Central University of Haryana

Shailja Singh
Jawaharlal Nehru University

Asif Mohmmed (amohd@icgeb.res.in)
International Centre for Genetic Engineering and Biotechnology

Pawan Malhotra (pawanmal@icgeb.res.in)
International Centre for Genetic Engineering and Biotechnology

Research Article

Keywords: Malaria, P. falciparum, Inner Membrane Complex, Merozoite invasion, Glideosome, Merozoite Reorientation

Posted Date: February 3rd, 2021

DOI: https://doi.org/10.21203/rs.3.rs-87875/v2

Plasmodium falciparum PhIL1 associated complex play an essential role in merozoite reorientation and invasion of host erythrocytes.

Ekta Saini[1], Pradeep Kumar Sheokand[1], Vaibhav Sharma[1], Prakhar Agrawal[1], Inderjeet Kaur[1,2#], Shailja Singh[3], Asif Mohmmed[1*] and Pawan Malhotra[1*]

[1]International Centre for Genetic Engineering and Biotechnology, New Delhi-10067, India.
[2]Department of Biotechnology, Central University of Haryana, Haryana-123031, India.
[3]Special Centre for Molecular Medicine, Jawaharlal Nehru University, New Delhi-110067, India

[#]Present affiliation

*Corresponding authors

Correspondence: Dr. Pawan Malhotra
Group leader, Malaria Biology Group, ICGEB, New Delhi
Email: pawanmal@gmail.com
Phone number: +91-11-26742895

Abstract

The human malaria parasite, *Plasmodium falciparum* possess a unique gliding machinery referred as glideosome that powers its entry into the insect and vertebrate hosts. A number of parasite proteins including Photosensitized INA-labelled protein 1 (PhIL1) have been shown to associate with glideosome machinery. Here we describe a novel PhIL1 associated protein complex that co-exists with glideosome motor complex in the inner membrane complex of the merozoite. Furthermore, using experimental genetics approach we characterized the role(s) of three proteins associated with PhIL1: a glideosome associated protein- PfGAPM2, an IMC structural protein- PfALV5 and a previously uncharacterised protein - referred here as PfPhIP (PhIL1 Interacting Protein). Parasites lacking PfPhIP or PfGAPM2 were unable to invade the host RBCs. Additionally, the down regulation of PfPhIP resulted in significant defects in merozoite segmentation. Furthermore, the PfPhIP and PfGAPM2 depleted parasites revealed abrogation of reorientation/gliding, however initial attachment with host RBCs was not affected in these parasites. Together, the data presented here shows that proteins of the PhIL1 associated complex plays an important role in orientation of *P. falciparum* merozoites following initial attachment, which is crucial for formation of tight junction and hence invasion of host erythrocytes. The identification and characterization of PhIL1 associated complex opens new avenues for future anti-malarial drug development.

Keywords: Malaria, *P. falciparum*, Inner Membrane Complex, Merozoite invasion, Glideosome, Merozoite Reorientation.

Significance Statement

Invasion of *Plasmodium* merozoites into RBCs is a multistep process that involves initial attachment of merozoites on RBC surface, their reorientation and subsequent gliding into RBCs using glideosome machinery. The Glideosome machinery lies between the plasma membrane and Inner membrane complex (IMC) and consists of MyoA, its interacting protein; MTIP, Gliding assocaited proteins (GAPs) and a Phosphoinositized INA labeled protein (PhIL1) associated complex. Here, we demonsrate that the deletion of two components; PfPhIP or PfGAPM2 of PhIL1 associated complex, aborts the merozoite reorientation and blocks their invasion into RBCs. The study thus provides new molecular and mechanistic insights into merozoite invasion of RBCs and opens avenues for identification of new molecules for intervention strategies for malaria parasite invasion and development.

Introduction

Invasion of *Plasmodium falciparum* merozoites during the asexual blood stages is a multistep process that involves initial contact, reorientation, active invasion by gliding motility and resealing [1]. All these steps are highly regulated and are mediated through a series of interactions from distinct *Plasmodium* and host proteins [1-4]. Successful invasion of human erythrocytes is thus essential for parasite survival and therefore is the target of malaria vaccine and inhibitor(s) development. One of the unique step in the invasion/egress of apicomplexan zoites including the *Plasmodium* merozoite is the gliding motility that powers parasites to cross non-permissive biological host membranes [5]. *P. falciparum* and *T. gondii* have a unique gliding machinery powered by actomyosin motor; the glideosome that brings about the gliding of zoites into the host and this glideosome is anchored to inner membrane complex (IMC) that is composed of flattened membrane cisternae or alveolar vesicles, whose cytoplasmic face is connected to subpellicular microtubules and a subpellicular protein network (SPN). The IMC of an *Apicomplexan* parasite plays diverse roles in maintaining structural stability of the zoite forms. It also acts as a scaffold for daughter cell development and plays a key role in motility and host-cell invasion. Proteins involved in the organization of pellicle/IMC/glideosome include structural proteins such as alveolins (IMC1a-h), glideosome associated protein- 40, -45 and -50 and glideosome associated proteins with multiple membrane spans (GAPMs), ISPs and these proteins together with MTIP (Myosin A tail domain interacting protein) anchor the actomyosin motor complex to the IMC [6, 7]. These structures and proteins of glideosome/IMC are important as any disruption in assembly of IMC, blocks parasite invasion as well as sexual stage development [8].

Despite these known IMC-associated protein families and complexes, the underlying functions of the IMC and its core complexes are still unexplored. We and others have shown that *Plasmodium* PhIL1 is localised to the IMC and is required for both asexual and sexual stages of parasite development [8, 9]. Gene disruption of PhIL1 prevented the formation of transmittable mature gametocytes [8]. Our analysis of PfPhIL1 interactome identified Alveolin (ALV5), glideosome associated proteins GAP50, GAPM1, -2 and -3 and few novel uncharacterized proteins such as PhIL1

interacting protein; PF3D7_1310700, PF3D7_1355600, PF3D7_1431100 and PF3D7_1430880.

In the present study, we selected three PhIL1 interacting proteins; a glideosome associated protein- PfGAPM2, an IMC structural protein- PfALV5 and a newly identified protein PF3D7_1310700- referred here as PfPhIP (PhIL1 interacting protein); and investigated the function of PhIL1 associated novel complex. Phenotypic analysis of parasites lacking PfGAPM2 and PfPhIP showed a role of these proteins in reorientation of *P. falciparum* merozoites that resulted in the disruption of invasion of human erythrocytes. The work thus identifies a novel PhIL1 associated protein complex and its role in reorientation of merozoite towards the host surface, a step essential for tight junction formation and subsequent invasion of merozoite into RBC.

Results

***P. falciparum* ALV5, PhIP and GAPM2 proteins co-localise with PhIL1 in the Inner membrane complex.**

To investigate the association of *P. falciparum* PhIL1 with other parasite proteins as shown in our previous interactome analysis [9], we expressed three proteins: a conserved protein of unknown function (PF3D7_1310700), referred here as PhIL1 Interacting Protein (PhIP); Alveolin 5 (PF3D7_1003600 or IMC1c); and GAPM2 (PF3D7_0423500) as GFP-tagged fusion protein in the parasite (Supplemental Fig S1A). Expression of fusion protein was confirmed by western blot analysis of lysate from the transgenic parasites using anti-GFP antibodies (Supplemental Fig S1B, C and D). Transgenic parasites expressing ALV5-GFP showed peripheral localisation in the schizont and merozoite stages (Fig 1A). Parasites expressing PhIP-GFP or GAPM2-GFP showed a similar pattern of peripheral localization in the IMC (Fig 1B and 1C). These proteins co-localised with PhIL1 in the IMC at schizont stage of the parasite with a Pearson's colocalization coefficient of more than 0.7 in an indirect immunofluorescence assay (Fig 1D).

Subsequently, we performed pull-down assays using GFP-Trap beads with the parasite extracts prepared from these transgenic lines. Immunoprecipitates were analysed by mass spectrometry to identify the interacting partners. The glideosomal

proteins GAP50, glideosome associated proteins with multiple membrane spans (GAPMs) 1, -2 and -3, and alveolin/ IMC protein family were identified in each precipitate, together with PhIP (PF3D7_1310700) and ALV5 (Fig 1E). Overall, these results confirmed the interactions among these proteins as well as with the PhIL1 protein.

PhIL1 associated novel complex is closely associated with the glideosomal complex.

To ascertain the existence of PhIL1 associated protein complex and its link with the glideosomal complex, if any, schizont stage parasite lysate was subjected to blue native PAGE followed by immunoblot analysis. As shown in Fig 2A, two bands; a high molecular weight band of ~800kDa and a low molecular weight complex of ~250kDa were observed, when gel was immunoblotted with anti-PhIL1 or anti-GAPM2 antibodies (Fig 2A). In comparison, anti-GAP50 or anti-PhIP or anti-ALV5 antibodies recognized a single band of ~800 kDa. These results indicated the involvement of PhIL1 and GAPM2 in two independent complexes that are composed of different but overlapping proteins.

To further substantiate these results, we performed sedimentation analysis of *P. falciparum* 3D7 schizont/ merozoite lysate using glycerol density gradient centrifugation. Western blot analysis of the glycerol gradient fractions revealed that PhIP, GAPM2, and ALV5 proteins co-sedimented together with PhIL1 in fractions 5 to 11, particularly in fraction 9 corresponding to ~250 kDa molecular mass (Fig 2B and supplemental Fig S2A-E), suggesting that these proteins probably are associated together in the parasite. *In-vitro* protein-protein interaction tool Far western blot analysis [10] provided additional evidence for the co-existence of PfPhIL1 and PfGAP50. We recombinantly expressed PfPhIL1 [9] and PfGAP50 proteins and performed far western blotting. Far western analysis strongly detected the interaction between membrane-bound recombinant PfGAP50 protein (Fig 2C and supplemental Fig S2F) and soluble recombinant PfPhIL1 bait protein (Fig 2D and supplemental Fig S2F).

Taken together, results presented here (Figs 1 and 2) validate the association of these proteins with each other, and in particular, their interactions with select, but not

all components of the glideosome machinery. The data thus illustrates that these proteins probably form an independent complex in the IMC, which may have a diverse role than the glideosome complex described earlier. Based on the above results, we propose that PhIL1 forms a novel complex probably in the outer IMC, having overlapping components with the glideosomal motility complex. The organisation of the proposed novel PhIL1 associated complex is depicted in Fig 2E.

PhIL1 associated complex plays an important role in parasite development and invasion.

To address the role of PfALV5, PfPhIP and PfGAPM2 proteins in *P. falciparum*, we generated conditional knock-down parasite lines expressing respective genes in fusion with HA-*glm*S. The *glm*S ribozyme is expressed downstream of the target gene, which is efficiently knocked down in response to glucosamine (GlcN). Strategy for generating the knock-down lines is presented in Supplemental Fig S3A. Integration into the parasite genome was confirmed by PCR analysis (Supplemental Fig S3B, C and D).

Expression and efficient knockdown of the fusion protein was analysed by western blot of lysate from transgenic parasites using anti-HA antibody under the effect of GlcN inducer (Fig 3A, D and G). Ring stage parasites at 16-20 hpi were treated with GlcN (2.5 mM), parasites were harvested at 42-44 hpi and the lysate was subjected to SDS-PAGE. PfBiP, a constitutively expressed endoplasmic reticulum chaperon protein was used as a loading control. Apparent knockdown of up to ~80-85% was achieved for the expression of ALV5-HA, PhIP-HA and GAPM2-HA in the respective parasite lysates.

GlcN was added at the ring stage parasites 16-20 hpi at varying concentrations (0.6 mM, 1.25 mM, 2.5 mM, and 5 mM) and the parasite growth was monitored till the formation of new rings i.e., up till one invasion cycle. Loss of ALV5 had little effect in the invasion of human RBCs by merozoites in comparison to the wild type parasites (Fig 3B), however PhIP depleted parasites showed ~80% invasion inhibition at 5 mM glucosamine (Fig 3E) while reduction in GAPM2 levels exhibited an invasion inhibitory potential of ~80% at 1.25 mM concentration of GlcN (Fig 3H).

Representative Giemsa-stained smears of the ALV5 knockdown parasites showed no significant difference apart from a slightly delayed parasite growth cycle in the GlcN treated (5 mM) and untreated parasites, suggesting that ALV5 is not essential for parasite growth (Fig 3C). In comparison, the PhIP-HA-*glm*S parasites showed arrested development of schizonts (1.25 mM GlcN treatment) (Fig 3F). In PhIP knockdown parasites two distinct phenotypes were observed; ~43% showed unsegmented merozoites, while 57% of the PhIP depleted schizonts, egressed normally, however, these merozoites were unable to invade and newly released merozoites were seen arrested on the surface of RBC suggesting that, despite the initial attachment, parasite was unable to penetrate the host RBC (Fig 3F-zoom and supplemental Fig S4). In the absence of GlcN, distinct merozoites were observed enclosed in all schizonts and these merozoites invaded normally as seen with their ability to progress to ring stage (Fig 3F). By contrast, treatment of GAPM2-HA-*glm*S with GlcN resulted in normal merozoite egress, however released merozoites were found to be stuck at erythrocyte surface, indicative of their inability to invade the RBC (Fig 3I).

PfPhIP knock-down results in underdeveloped IMC during schizogony leading to defective segmentation of daughter merozoites.

We further dissected the defects in merozoite segmentation in PfPhIP knock-down parasites for the formation of the parasite plasma membrane (PPM), formation of and secretion by apical secretory organelles and IMC formation using immunostaining. Briefly, schizonts maintained with and without GlcN from the early ring-stage were treated with 10 µM E64 at 42 hpi, to prevent release of daughter merozoites. In PhIP depleted parasites, multiple daughter cells remained partially attached to each other. In these parasites, segmented merozoites showed residual signal for PfPhIP, whereas in the unsegmented agglomerate PfPhIP staining was not detected (Fig 4A). PhIP depleted parasites showed apparent loss of signal for GAP50 in the multi-nucleated agglomerates suggesting defect in IMC formation in agglomerates while [-] GlcN parasites, showed well-formed IMC around each nucleus of the segmented schizont (Fig 4B). Parasite plasma membrane which coats the individual newly formed daughter cells was examined by Merozoite Surface Protein 1 (MSP1). PhIP depleted schizonts showed MSP1 staining enclosing

multiple nuclei of the agglomerate inside one contiguous membrane in contrast to untreated parasites that showed MSP1 surrounding each segmented daughter merozoite nucleus discretely (Fig 4C and Supplemental Fig S5A). Thus, in the agglomerates, PhIP knock-down parasites failed to direct the PPM around single daughter nuclei. Simultaneously, microneme formation and secretion was assessed using anti-PfAMA1 (Apical Membrane Antigen 1) antibody in [-] GlcN as well as [+] GlcN parasites. Following the egress trigger, apical membrane antigen 1 (PfAMA1) is translocated from micronemes to the merozoite membrane. [-] GlcN PhIP-HA*glmS* parasites showed AMA1 staining around each merozoite, whereas PhIP depleted parasites demonstrated surface AMA1 staining in fully segmented merozoites, while loss of AMA1 signal on merozoite surface was observed for the multi-nucleated agglomerates (Fig 4D and Supplemental Fig S5B). 3D reconstruction of schizont stage transgenic parasites with and without GlcN with respect to different marker antibodies is illustrated using Imaris, version 7.6.1 (Fig 4E).

The ultra-structure of this incomplete budding in E64-treated schizonts with and without GlcN was examined by electron microscopy (Fig 4F). As expected, in the absence of GlcN, we observed distinct membrane enclosed merozoites with organised rhoptries. In the presence of GlcN, only few merozoites were separated from each other and a multi-nucleated agglomerate of unsegmented merozoites with randomly placed sets of organelles was present close to the food vacuole.

These results established that PfPhIP-deficient parasites show developmental defect during the final stages of schizont segmentation that fail to reinstate the asexual blood cycle due to structural defects.

PfPhIP and PfGAPM2 knock-down results in generation of non-invasive merozoites.

Since we observed that the merozoites formed in PfPhIP and GAPM2 knock-down parasites were able to attach to the RBC surface, but could not invade, we next performed immunostaining of these RBC attached but non-invasive merozoites, to determine whether the inability of merozoites to invade the RBCs is due to defects in apical organelles biogenesis or their secretion, which is crucial for formation of invasion complex; or due to the inability of motility complex which fails to propel the

invading merozoite into the host RBC. To understand whether the IMC formation is affected in these knock-down parasites, we stained these attached merozoites with anti-PfGAP50 antibody. PhIP deficient merozoites showed loss of signal for GAP50 suggesting defects in IMC formation (Fig 5A; panel 1) while GAPM2 depleted merozoites displayed intact IMC encircling the nascent attached merozoite (Fig 5B; panel 1). To assess the merozoites released from the PhIP or GAPM2 deficient schizonts for the formation and secretion of apical organelles, we used EBA175, and AMA1 as markers for micronemes, and PfRON2 as a rhoptry marker. We observed typical micronememal staining as visualized by the presence discrete dots with anti-EBA175 and anti-AMA1 antibodies. However, we could not locate these proteins on merozoite surface in the merozoites released from the PhIP and GAPM2 knockdown schizonts, therefore indicating the failure to discharge the micronemal contents post egress (Fig 5A and B; panel 2 and 3). We additionally evaluated the presence of PfRON2, a rhoptry marker in merozoites in PfPhIP- and PfGAPM2-knockdown parasites. These knock-down parasites displayed characteristic rhoptry and micronemal localisation (Fig 5A and B; panel 3). Following the egress, PfAMA1 is known to translocate from micronemes to the merozoite membrane and PfRON2 is inserted into the host membrane [11]. Together, these results indicated that merozoites formed and released in PfPhIP- and PfGAPM2-knockdown parasites were morphologically normal. However, apical organelle secretion of the invasion ligands seems to be affected in the merozoites released from schizonts with PfPhIP and PfGAPM2 deficiency (Fig 5A and B; panel 3 and Supplemental Fig S6A and B). 3D reconstruction of stuck merozoites from transgenic parasites in presence of GlcN with respect to different marker antibodies are illustrated using Imaris, version 7.6.1 (Fig 5C).

Since the secretion of EBA175, AMA1, and RON2, failed to initiate following merozoite attachment in PfPhIP- and PfGAPM2-deficient merozoites, it clearly suggested that the signal for invasion in these merozoites post attachment to the erythrocytes was not triggered in PfPhIP- and PfGAPM2-knockdown parasites. On detailed analysis, we observed ~87% of the attached merozoites failed to align their apical end towards the erythrocyte surface i.e., the apex of the merozoite is not in direct proximity of the erythrocyte surface as indicated by staining with apical marker proteins. Apical reorientation is imperative for triggering commitment to invasion.

Taken together, the analysis of attached PfPhIP- and PfGAPM2-deficient merozoites suggested role of PfPhIP and GAPM2 in the reorientation of merozoites so that the apical organelles are aligned to the erythrocyte membrane (Fig 6). This study also highlights that merozoite reorientation might directly or indirectly mediated by the motor complex due to existence of the overlapping components among these two complexes.

Discussion

A unifying feature of apicomplexan parasites is the presence of a surface pellicle and highly polarised cellular organisation with the apical complex at the anterior end of their invasive stages, which is implicated in motility and invasion of host cells/tissue [12]. IMC acts as an anchor for motor complex, playing significant role in gliding and thus invasion [5, 13]. A number of studies have identified several proteins associated with the IMC and have provided insights into the organisation and roles of the glideosome complex [5, 14-16]. The basic motor complex in apicomplexan parasites that drives gliding motility and invasion is comprised of conserved components such as actin-MyoA-MTIP-GAP45-GAP40-GAP50-GAPMs-aldolase. IMC has also been implicated to be involved in cell division [15].

Earlier, we and others have shown *Plasmodium* PhIL1 to be localised in parasite IMC and its association with alveolins and other protein components that overlap with those in the known glideosome complex, including GAP50 [8, 9]. In the present study, we show the existence of PhIL1 associated complex and delineate the functional relevance of PhIL1 associated novel proteins in the *P. falciparum* merozoite namely, IMC1c or ALV5, a structural constituent of the SPN; a previously uncharacterised protein, PF3D7_1310700, which we termed PhIL1 Interacting Protein (PhIP); and GAPM2, a well-established component of the glideosomal complex. GFP tagged proteins of PhIP, ALV5 and GAPM2 confirmed their localisation to the IMC and co-localisation studies using indirect immunofluorescence assay affirmed the close association of these proteins with PhIL1 in asexual blood stage of the parasite. The alliance amongst these proteins were also established by reciprocal co-precipitation studies using GFP-Trap wherein GFP tagged proteins from all the three parasite lines (ALV5-, PhIP- and GAPM2-GFP) were co-

precipitated with their interacting protein partners and components of the PhIL1 associated complex.

Blue-native PAGE and co-sedimentation analysis of schizont stage parasite extracts confirmed the existence of PhIL1 and its associated proteins in complex(s). We could identify two discrete complexes; a low molecular mass complex corresponding to ~250kDa having PhIL1 and GAPM2 proteins and a high molecular weight complex of ~800kDa consisting of ALV5, PhIP, GAPM2, PhIL1 and GAP50, indicating the heterogeneity among these two complexes, which are composed of different but overlapping proteins. These results suggested a possible association of PhIL1 associated complex with the glideosomal complex. Far western assay using recombinant PhIL1 and GAP50 additionally confirmed the interaction between the two proteins and thus confirming GAP50 as the link between the two complexes. It is conceived that the motor complex assembles at the N-terminus of the GAP50 anchor [17]. It is possible that GAPM proteins, which span both the outer and inner side of the IMC, may be part of different complexes on either side of the IMC. Therefore, we speculate that PhIL1 associates with GAP50 at the other end of the IMC i.e., at its C-terminus along with GAPMs and alveolins [18] and is a part of a novel complex at the inner IMC. Since GAP50 is both a luminal and transmembrane protein, it is possible that PhIL1 associated complex interacts with GAP50 on the inner membrane of the IMC and GAP50 interacts on the outer side with the myosin machinery like GAP45, GAP40, MyoA and MTIP [19-21].

We next characterised these selected components of the PhIL1 associated complex using conditional knock-down approaches. *Plasmodium* alveolins are thought to be involved in parasite motility through interactions with the pellicular membrane embedded glideosomal components, apart from their role in morphogenesis and providing tensile strength. The conditional knockdown of PfALV5 slightly delayed the developmental time span at late stages of the asexual cycle, although the parasite could complete its growth leading to the formation of new rings. This could be due to the redundancy among 13 members of the alveolin family. These results are in line with *Pb*IMC1d knock-out study where no apparent phenotype was observed [22]. Even a double knockout of alveolins (IMC1b and IMC1h) revealed decreased tensile strength of ookinetes without affecting their morphology [23]. It appears that

glideosomal associated protein complexes exhibit considerable plasticity in their functions to ensure survival of the parasite. MyoA is reported to be recruited at the apical cap of the parasite through interactions with GAP45 or its paralog GAP70. Another member of this family, GAP80 recruits and assembles a new glideosome with MyoC at the basal polar region. Both these complexes share GAP50, GAP40 and MTIP. It was found that the deletion of MyoA is compensated by MyoC as it relocates to the apical end to initiate invasion and vice-versa [24]. These studies emphasize on high degree of complexity and functional versatility of the IMC components involved in gliding. Similar compensatory mechanisms have been reported for GAP45 and its ortholog at the basal region [13]. Recent investigations have demonstrated that parasite can invade the host cell in the absence of several core components of the glideosomal machinery (such as MyoA, MIC2, MLC1, GAP45 and actin), indicating the existence of an alternative motor mechanisms for invasion [19-21]. All these studies uncover the fact that until now what was considered to be as a highly conserved machinery exhibits different protein complexes sharing some common components and displays complementary and compensatory mechanisms for successful invasion.

In contrast to the knock-down results for ALV5 parasites, PhIP and GAPM2 knock-down parasites showed pronounced effect on parasite invasion. Following PhIP knockdown, a proportion of schizonts displayed incomplete segmentation and multiple merozoites remained attached to each other, while distinct merozoites were observed enclosed in schizonts in wild type parasites as shown by light, immunofluorescence and electron microscopy. This resultant phenotype might be due to the failure of IMC biogenesis and stabilisation. Similar phenotype had been observed in case of Merozoite Organising Protein (PfMOP) knock-down parasites, where agglomerates were noted due to flawed segmentation [25]. Also, this is in agreement with PfSortilin knockdown study that showed involvement of Sortilin in IMC biogenesis [26]. Together, the data suggested a possible role of PfPhIP in IMC formation in maturing schizonts and failure to do so results in the absence of plasma membrane enclosing individual daughter merozoites in the agglomerates. Similar observations have been reported upon depletion of GAP40 and GAP50, which resulted in defective IMC biogenesis and stabilisation during replication [14].

Some of the PhIP depleted schizonts were fully segmented and generated merozoites which egressed normally, however the merozoites released from these schizonts unable to invade host RBCs and got arrested on the surface of RBCs. These results suggest that, despite the initial attachment, merozoites were unable to penetrate the host RBC, which might be due to impaired reorientation of the invading merozoites. The two distinct phenotypes observed due to ablation of PhIP, demonstrates the divergent functions of the components of IMC during asexual lifecycle of the parasite. Recent work has provided evidence that specific proteins of the IMC can independently be involved in both motility and maintenance of cell shape and strength [23]. We speculate that PhIP might play a dual role in maintaining the cellular integrity of the daughter cells during cell division along with its role in reorientation of merozoites during the invasion process.

The conditional knock down of GAPM2-HA-glmS parasites showed the inability of merozoites to invade the RBCs. However, it was observed that the attachment of invasive merozoite is not affected in these parasites. While, untreated GAPM2-HA-*glm*S parasites progressed to ring stage infection. A recent study highlighted the role of GAPM1 and GAPM3 in providing the bridge between the sub-pellicular network and the alveoli in the IMC in order to maintain parasite structure and rigidity. GAPM1 depletion resulted in depolymerization of microtubules compromising parasite shape and integrity [27]. However, there has been no report suggesting the role of GAPMs in invasion of the host.

Merozoite invasion is a complex, multistep process. First, there is a reversible attachment of merozoite to the erythrocyte surface through any part of the merozoite surface i.e. the apex of the merozoite is not in direct proximity of the erythrocyte surface followed by its apical reorientation so that the apical organelles are aligned to the erythrocyte membrane, formation of an irreversible tight junction (primarily involving AMA1 and RON) and ultimately its entry into the host cell powered through the motor complex. These steps are timed by organelle secretion and various signaling events [1]. To get insight into the defects in invasion of merozoites released from PfPhIP and PfGAPM2 knockdwon schizonts, we assesed the expression and secreation of the invasion ligands using EBA175, AMA1 and RON2. Post egress, AMA1 is exported from micronemes to the parasite surface and the secreted Rhoptry

neck protein RON2 is inserted in the erythrocyte membrane, which binds to AMA1 on the merozoite surface which leads to the formation of tight junction committing the merozoite to invade the host [11]. Despite showing expected expression pattern for the apical organelles, the release of these invasion ligands onto the merozoite surface appeared to be affected. These defects in organelle secretion were found to be due to failure of the attached merozoites to reoreint their apical end towards the RBC surface; which in turn triggers the signaling events for the release of contents from apical organelles. The specific molecular interactions and mechanisms involved in apical reorientation are poorly understood. Till date, there is no evidence for the involvement of Glideosome or its associated motor protein complexes in mediating the reorientation of apical organelles of the merozoites towards the host surface. A study (bioRxiv Preprint) recently identified the gliding ability of *Plasmodium* merozoites facilitated by actomyosin motor [28]. Data presented here suggests the role of PfPhIP and PfGAPM2 in the reorientation which might be directly or indirectly mediated through motor complex in *P. falciparum* merozoites.

In Conclusion, we have characterised *P. falciparum* ALV5; PhIP, a previously uncharacterised protein; and GAPM2 and show that GAPM2 and PhIP are essential for the blood stage infection and their genetic attenuation arrests merozoite invasion resulting from the failure of merozoite to reorient its apical end towards the host RBC (Fig 6). Taken together, our results suggest that PhIL1 associated IMC complex is different in composition with that of previously described glideosomal complex and it appears to be essential for parasite invasion of erythrocytes. The study thus provides new molecular and mechanistic insights into contribution of IMC which will likely be effective in identifying new molecules for intervention strategies for malaria parasite development.

Experimental Procedures

Maintenance of *P. falciparum* cultures

P. falciparum parasite line 3D7 was maintained in O^+ human erythrocytes (RBC) at 3% hematocrit in RPMI 1640 medium (pH 7.4) supplemented with 50 µg/ml hypoxanthine, 0.5% albumax II, 2 mg/ml sodium bicarbonate, and 20 µg/ml gentamycin. Cultures were incubated in air tight boxes at 37 °C in an atmosphere of

1% O_2, 4% CO_2 and 95% N_2 [29]. Parasites were synchronized using sorbitol treatment [30]. Briefly, the culture was harvested at about 10 % parasitemia with majority of parasites at the ring stage by centrifuging at 2000 rpm for 5 min at RT. To the cell pellet, 5 volumes of 5 % sorbitol solution was added and mixed gently. This solution was incubated at 37ºC for 10 min and centrifuged at 2000 rpm for 5 min. The supernatant was carefully discarded without disturbing the pellet. Pellet was washed with prewarmed complete media twice and the culture was incubated at 37ºC for the growth of the parasite.

P. falciparum parasite transfection

To generate a GFP-tagged transfection vector construct, the entire open reading frame of PfPhIP, PfALV5, and PfGAPM2 was amplified using gene specific primers (Supplemental Table 1) and cloned into the transfection vector pSSPF2 [31] at the *Bgl*II and *Avr*II restriction sites to create a fusion of desired gene of interest (GOI) with GFP under the control of the *hsp86* promoter. Synchronized *P. falciparum* 3D7 ring stage parasites were transfected with 100 µg of purified plasmid DNA by electroporation (310 V, 950 µF) and the transfected parasites were selected using 2.5 nM blasticidin [32]. To detect expression of the PfGOI-GFP fusion protein in the transgenic line, parasite lysates were analysed with western blotting using anti-GFP antibody.

For the generation of knock-down constructs, C-terminal region of PfPhIP, PfALV5, and PfGAPM2 was amplified using gene specific primers (Supplemental Table S1) and cloned into the transfection vector pHA-glmS [33] using *Pst*I and *Bgl*II restriction sites to create a fusion of desired gene of interest (GOI) with HA-glmS under the control of native promoter. The ring stage parasites were transfected as mentioned and transgenic parasites were selected on alternate blasticidin drug ON and OFF cycles to ensure genomic integration of PfGOI-HA-glmS constructs. The transgenic parasites were then subjected to clonal selection by serial dilution to obtain parasite line from a single genome integrated clone.

Isolation of parasites, extraction of proteins and immunoblotting

Expression of the PfGOI-GFP or PfGOI-HA fusion protein in transgenic *P. falciparum* blood stage parasites was examined by western blotting as described previously [9].

Briefly, schizont stage parasites were isolated following lysis of infected erythrocytes with 0.15% saponin; following centrifugation the pellet was resuspended in RIPA buffer (150 mM NaCl, 1% Nonidet P-40, 0.5% sodium deoxycholate, 0.1% SDS, 50 mM Tris pH 8.0) and cells were lysed at 4ºC for 30 min, followed by 3 cycles of freeze-thaw in liquid N_2 and at 37ºC. A clear parasite lysate was obtained by centrifugation at 13,000 rpm for 30 min at 4ºC. The supernatant was then mixed with Laemmli buffer, boiled and centrifuged, and proteins were separated on 12% SDS-PAGE. The fractionated proteins were transferred from the gel on to the PVDF membrane (Millipore) for 2 h at 200 mA and then the membrane was treated with blocking buffer (5% milk powder in 1 × PBS) overnight at 4ºC. The blot was incubated for 1 h with rabbit anti-GFP (1: 10,000) or rat anti-HA (1:1000), followed with secondary anti-rabbit/anti-rat IgG antibody (1: 300,000) conjugated to HRP. Protein bands were visualized using an ECL detection kit (Thermo Scientific, USA).

Fluorescence microscopy

To visualize GFP expression, the transgenic parasite suspension was incubated with DAPI (2 ng/ml) in PBS at RT for 10 min. Following three washes with 1 × PBS (pH 7.4); samples were mounted on glass slides and observed on a Nikon A1 Confocal Microscope (Nikon Corporation, Tokyo, Japan).

Indirect Immunofluorescence Assay

Parasites were fixed with fixation solution containing 4% paraformaldehyde and 0.0075% glutaraldehyde in PBS for 30 min and subjected to permeabilization with 0.1% Triton X-100 followed by blocking with 10% FBS. Parasites were then probed with primary antibody for 1 h, followed by secondary antibody for 1 h at RT. The parasites were incubated with DAPI to stain the nucleus for 10 min at RT and imaged using a Nikon A1-R confocal microscope (Nikon Corporation, Tokyo, Japan). The images were analysed by NIS elements software (Nikon). The antibody combinations used for various experiments are: 1. For colocalization with the GFP line, rabbit α-PfPhIL1 (1:100) was used, 2. For the colocalization studies in knockdown experiments, rabbit α-PfGAP50 (1:100), rabbit anti-PfMSP1 (1:250), rabbit α-PfAMA1 (1:100), rabbit α-PfEBA175 (1:100), mice α-PfRON2 (1:50) and rat α-HA (1:100) were used; followed by appropriate secondary antibodies: anti-mice

Alexafluor 488 (1:500), anti-rabbit Alexafluor 488 (1:500), anti-rabbit Alexafluor 594 (1:500), and anti-rat Alexafluor 488 (1:500) (Invitrogen).

Conditional knock down assay

The functional role of PfALV5, PfPhIP and PfGAPM2 was determined by inducible knock down with glucosamine. Glucosamine was added to the parasite lines (PfGOI-HA-glmS transgenic and 3D7) with a haematocrit and parasitaemia of synchronized ring stage culture adjusted to 2% and 1%, respectively, at varying concentrations (0.3 mM, 0.6 mM, 1.25 mM, 2.5 mM, and 5 mM). Parasite growth was monitored microscopically after every 8 h by Giemsa-stained smears. The parasitaemia was estimated after an incubation of 40 h in the next cycle and percent inhibition was calculated relative to the GlcN untreated PfGOI-HA-glmS parasite cultures. Briefly, cells from samples were collected and washed with PBS followed by staining with ethidium bromide (10 µg/ml) for 20 min at 37°C. The cells were subsequently washed twice with PBS and analysed on FACSCalibur (Becton Dickinson) using the Cell Quest Pro software. Fluorescence signal (FL2) was detected with the 590 nm band pass filter using an excitation laser of 488nm collecting 100000 cells per sample. Uninfected RBCs stained in similar manner were used as control.

Co-precipitation of interacting proteins

For Pull-down of GFP-fusion proteins, schizont stage lysate was obtained as described above and immunoprecipitation was done using GFP-Trap®_A Kit (Chromotek) following the manufacturer's instructions. GFP-Trap®_A beads were equilibrated with dilution buffer and allowed to bind to proteins in the parasite lysate by tumbling the tube end-over-end for 3 h at 4ºC. Samples were then centrifuged at 1600 rpm for 1 min and the beads washed twice with dilution buffer. Proteins were eluted in 50 µl elution buffer and peptides were analysed by mass spectrometry.

Glycerol Density Gradient fractionation for isolation of complexes

The sedimentation curve of molecular mass standards in different fractions and the protocol followed is as described earlier [34]. Briefly, schizont stage parasites were lysed as described above. Lysate was cleared by centrifugation, and 500µLof lysate

was layered on top of a 9 mL 5-45% glycerol step-gradient (45% glycerol solution being the lowermost and 5% glycerol solution being the topmost layer). Gradients were centrifuged at 38,000 rpm for 18 h at 4°C in a SW41 Ti rotor (Beckman). Twenty, 0.5 mL fractions were collected from each gradient, and equal volumes of each fraction was mixed with sample loading dye. Alternate protein fractions were resolved by SDS/PAGE and analysed by Western blotting using protein specific antibodies at 1:5000 dilution for GAP50, PhIL1, ALV5, PhIP and GAPM2 followed by secondary α-rabbit antibody at 1:100000 dilution and detection using an ECL detection kit (Thermo Scientific, USA).

Native gel electrophoresis

Native-PAGE analysis was carried out to separate various complexes present in the parasite lysate using NativePAGE™ Novex® Bis-Tris Gel System (Life technologies) following manufacturer's protocol. Briefly, Schizont stage parasite lysate was mixed with NativePAGE sample buffer and NativePAGE 5% G-250 sample additive, and resolved in the NativePAGE™ Novex® 4–16% Bis-Tris Gels at 4°C, which resolve proteins in the molecular weight range of 15-1,000 kDa and then transferred to polyvinylidene difluoride (PVDF) membranes. To identify PfPhIL1 associated complexes, membrane was probed with rabbit anti-PfGAP50, anti-PfPhIL1, anti-PfALV5, anti-PfPhIP and anti-PfGAPM2 (1:5000 dilution each) antisera, followed by incubation with HRP-conjugated goat anti-rabbit IgG secondary antibody (1:100,000).

Transmission electron microscopy.

PfPhIP-HAglmS parasites [+]/ [-] GlcN were percoll purified at 42 hpi and treated with 10 µM E64. Parasites were washed in phosphate buffer (pH 7.0) and fixed with 1% paraformaldehyde. [-] GlcN parasites were fixed at 48 hpi and [+] GlcN parasites were fixed at 52 hpi. Parasites were then resuspended in 2.5% glutaraldehyde followed by addition of 2% Osmium Tetroxide and washed with phosphate buffer. The samples were then subjected to subsequent dehydration in grades of alcohol (50%, 60%, 70%, 80%, 90% and 100%). The samples were then infiltrated in Epoxy resin composed of ERL-4221, DER 736, DMAE, and NSA (Ted Pella, Inc). The following day, samples were embedded in Epoxy resin and baked at 65ºC for 16h.

Ultrathin sections (about 90nm) were cut on ultramicrotome RMC Boeckeler PTPC, samples were stained using lead citrate followed by 1% Uranyl acetate, visualized in Tecnai G2 spirit (FEI, Netherland), operating at a voltage of 120kV, and images were recorder with a Mega View III (SIS, Germany) digital camera.

Far western blotting

Far western assay was carried out according to the protocol described by Xing-Zhen Chen and colleagues [10].

Author Contributions: Conceptualization, P.M., A.M., and E.S.; Writing – P.M., A.M., and E.S.; Intellectual input, illustrations, and scientific discussions, P.M., A.M., E.S. and P.K.S.; E.S., P.K.S., and V.S. conducted the experiments; S.S. optimised EM staining; I.K. performed the mass spectroscopy; Funding Acquisition, P.M., and A.M.

Acknowledgements: ES acknowledges the financial support from Department of Biotechnology, Government of India in the form of DBT-JRF Fellowship. PKS and VS are awardees of fellowship from University Grants Commission (UGC) and Council of Scientific & Industrial Research (CSIR), Govt. of India, respectively. We thank Rotary blood bank, for providing packed red blood cells. We thank Dr. Chetan E. Chitnis and Dr. Mansoor A Siddiqui for providing PfAMA1 and PfEBA175 antibodies. We are grateful to Paul Gilson for providing vector pHA-*glm*S and Siggi Sato for pSSPF2 vector. We acknowledge the support of Dr. Tenzin Choedon for electron microscopy imaging. The research work in PM's and AM's laboratory is supported by Flagship Project (BT/IC-06/003/91), Indo-Danish grant (BT/PR5267/MED/15/87/2012) and Centre of Excellence grant (BT/COE/34/SP15138/2015) from Department of Biotechnology, Govt. of India. PM is recipient of J C Bose Fellowship awarded by SERB, Govt. of India (SERB/F/4675/2020). The funders had no role in the design of the study and collection, analysis, and interpretation of data and in writing the manuscript.

Disclosure of Interest: The authors declare no competing interests.

References

1. Cowman AF, Berry D, Baum J. The cellular and molecular basis for malaria parasite invasion of the human red blood cell. The Journal of cell biology. 2012;198(6):961-71. Epub 2012/09/19. doi: 10.1083/jcb.201206112. PubMed PMID: 22986493; PubMed Central PMCID: PMCPMC3444787.

2. Gaur D, Mayer DC, Miller LH. Parasite ligand-host receptor interactions during invasion of erythrocytes by Plasmodium merozoites. Int J Parasitol. 2004;34(13-14):1413-29. PubMed PMID: 15582519.

3. Harvey KL, Gilson PR, Crabb BS. A model for the progression of receptor-ligand interactions during erythrocyte invasion by Plasmodium falciparum. Int J Parasitol. 2012;42(6):567-73. PubMed PMID: 22710063.

4. Weiss GE, Gilson PR, Taechalertpaisarn T, Tham WH, de Jong NW, Harvey KL, et al. Revealing the sequence and resulting cellular morphology of receptor-ligand interactions during Plasmodium falciparum invasion of erythrocytes. PLoS Pathog. 2015;11(2):e1004670. Epub 2015/02/28. doi: 10.1371/journal.ppat.1004670 PPATHOGENS-D-14-01253 [pii]. PubMed PMID: 25723550.

5. Boucher LE, Bosch J. The apicomplexan glideosome and adhesins - Structures and function. Journal of structural biology. 2015;190(2):93-114. doi: 10.1016/j.jsb.2015.02.008. PubMed PMID: 25764948; PubMed Central PMCID: PMC4417069.

6. Poulin B, Patzewitz EM, Brady D, Silvie O, Wright MH, Ferguson DJ, et al. Unique apicomplexan IMC sub-compartment proteins are early markers for apical polarity in the malaria parasite. Biology open. 2013;2(11):1160-70. doi: 10.1242/bio.20136163. PubMed PMID: 24244852; PubMed Central PMCID: PMC3828762.

7. Daher W, Soldati-Favre D. Mechanisms controlling glideosome function in apicomplexans. Curr Opin Microbiol. 2009;12(4):408-14. Epub 2009/07/07. doi: 10.1016/j.mib.2009.06.008. PubMed PMID: 19577950.

8. Parkyn Schneider M, Liu B, Glock P, Suttie A, McHugh E, Andrew D, et al. Disrupting assembly of the inner membrane complex blocks Plasmodium falciparum sexual stage development. PLoS Pathog. 2017;13(10):e1006659. Epub 2017/10/07. doi: 10.1371/journal.ppat.1006659. PubMed PMID: 28985225; PubMed Central PMCID: PMCPMC5646874.

9. Saini E, Zeeshan M, Brady D, Pandey R, Kaiser G, Koreny L, et al. Photosensitized INA-Labelled protein 1 (PhIL1) is novel component of the inner membrane complex and is required for Plasmodium parasite development. Sci Rep. 2017;7(1):15577. Epub 2017/11/16. doi: 10.1038/s41598-017-15781-z. PubMed PMID: 29138437; PubMed Central PMCID: PMCPMC5686188.

10. Wu Y, Li Q, Chen XZ. Detecting protein-protein interactions by Far western blotting. Nat Protoc. 2007;2(12):3278-84. Epub 2007/12/15. doi: 10.1038/nprot.2007.459. PubMed PMID: 18079728.

11. Besteiro S, Dubremetz JF, Lebrun M. The moving junction of apicomplexan parasites: a key structure for invasion. Cellular microbiology. 2011;13(6):797-805. Epub 2011/05/04. doi: 10.1111/j.1462-5822.2011.01597.x. PubMed PMID: 21535344.

12. Morrissette NS, Sibley LD. Cytoskeleton of apicomplexan parasites. Microbiol Mol Biol Rev. 2002;66(1):21-38; table of contents. Epub 2002/03/05. doi: 10.1128/mmbr.66.1.21-38.2002. PubMed PMID: 11875126.

13. Frenal K, Polonais V, Marq JB, Stratmann R, Limenitakis J, Soldati-Favre D. Functional dissection of the apicomplexan glideosome molecular architecture. Cell Host Microbe. 2010;8(4):343-57. doi: 10.1016/j.chom.2010.09.002. PubMed PMID: 20951968.

14. Harding CR, Egarter S, Gow M, Jimenez-Ruiz E, Ferguson DJ, Meissner M. Gliding Associated Proteins Play Essential Roles during the Formation of the Inner Membrane Complex of Toxoplasma gondii. PLoS Pathog. 2016;12(2):e1005403. doi: 10.1371/journal.ppat.1005403. PubMed PMID: 26845335; PubMed Central PMCID: PMCPMC4742064.

15. Harding CR, Meissner M. The inner membrane complex through development of Toxoplasma gondii and Plasmodium. Cellular microbiology. 2014;16(5):632-41. doi: 10.1111/cmi.12285. PubMed PMID: 24612102; PubMed Central PMCID: PMC4286798.

16. Jacot D, Tosetti N, Pires I, Stock J, Graindorge A, Hung YF, et al. An Apicomplexan Actin-Binding Protein Serves as a Connector and Lipid Sensor to Coordinate Motility and Invasion. Cell Host Microbe. 2016;20(6):731-43. doi: 10.1016/j.chom.2016.10.020. PubMed PMID: 27978434.

17. Baum J, Richard D, Healer J, Rug M, Krnajski Z, Gilberger TW, et al. A conserved molecular motor drives cell invasion and gliding motility across malaria life

cycle stages and other apicomplexan parasites. The Journal of biological chemistry. 2006;281(8):5197-208. doi: 10.1074/jbc.M509807200. PubMed PMID: 16321976.

18. Bullen HE, Tonkin CJ, O'Donnell RA, Tham WH, Papenfuss AT, Gould S, et al. A novel family of Apicomplexan glideosome-associated proteins with an inner membrane-anchoring role. The Journal of biological chemistry. 2009;284(37):25353-63. Epub 2009/06/30. doi: 10.1074/jbc.M109.036772. PubMed PMID: 19561073; PubMed Central PMCID: PMCPMC2757237.

19. Andenmatten N, Egarter S, Jackson AJ, Jullien N, Herman JP, Meissner M. Conditional genome engineering in Toxoplasma gondii uncovers alternative invasion mechanisms. Nat Methods. 2013;10(2):125-7. Epub 2012/12/25. doi: 10.1038/nmeth.2301. PubMed PMID: 23263690; PubMed Central PMCID: PMCPMC3605914.

20. Egarter S, Andenmatten N, Jackson AJ, Whitelaw JA, Pall G, Black JA, et al. The toxoplasma Acto-MyoA motor complex is important but not essential for gliding motility and host cell invasion. PLoS One. 2014;9(3):e91819. Epub 2014/03/19. doi: 10.1371/journal.pone.0091819. PubMed PMID: 24632839; PubMed Central PMCID: PMCPMC3954763.

21. Shen B, Sibley LD. Toxoplasma aldolase is required for metabolism but dispensable for host-cell invasion. Proc Natl Acad Sci U S A. 2014;111(9):3567-72. Epub 2014/02/20. doi: 10.1073/pnas.1315156111. PubMed PMID: 24550496; PubMed Central PMCID: PMCPMC3948255.

22. Al-Khattaf FS, Tremp AZ, Dessens JT. Plasmodium alveolins possess distinct but structurally and functionally related multi-repeat domains. Parasitology research. 2015;114(2):631-9. Epub 2014/12/06. doi: 10.1007/s00436-014-4226-9. PubMed PMID: 25475193; PubMed Central PMCID: PMCPMC4303705.

23. Tremp AZ, Dessens JT. Malaria IMC1 membrane skeleton proteins operate autonomously and participate in motility independently of cell shape. The Journal of biological chemistry. 2011;286(7):5383-91. doi: 10.1074/jbc.M110.187195. PubMed PMID: 21098480; PubMed Central PMCID: PMC3037651.

24. Frenal K, Marq JB, Jacot D, Polonais V, Soldati-Favre D. Plasticity between MyoC- and MyoA-glideosomes: an example of functional compensation in Toxoplasma gondii invasion. PLoS Pathog. 2014;10(10):e1004504. Epub 2014/11/14. doi: 10.1371/journal.ppat.1004504. PubMed PMID: 25393004; PubMed Central PMCID: PMCPMC4231161.

25. Absalon S, Robbins JA, Dvorin JD. An essential malaria protein defines the architecture of blood-stage and transmission-stage parasites. Nat Commun. 2016;7:11449. Epub 2016/04/29. doi: 10.1038/ncomms11449. PubMed PMID: 27121004; PubMed Central PMCID: PMCPMC4853479.

26. Hallee S, Boddey JA, Cowman AF, Richard D. Evidence that the Plasmodium falciparum Protein Sortilin Potentially Acts as an Escorter for the Trafficking of the Rhoptry-Associated Membrane Antigen to the Rhoptries. mSphere. 2018;3(1). Epub 2018/01/05. doi: 10.1128/mSphere.00551-17. PubMed PMID: 29299530; PubMed Central PMCID: PMCPMC5750388.

27. Harding CR, Gow M, Kang JH, Shortt E, Manalis SR, Meissner M, et al. Alveolar proteins stabilize cortical microtubules in Toxoplasma gondii. Nat Commun. 2019;10(1):401. Epub 2019/01/25. doi: 10.1038/s41467-019-08318-7. PubMed PMID: 30674885; PubMed Central PMCID: PMCPMC6344517.

28. Kazuhide Yahata MNH, Heledd Davies, Masahito Asada, Thomas J. Templeton, Moritz Treeck, Robert W. Moon, Osamu Kaneko. Gliding motility of Plasmodium merozoites. bioRxiv Preprint. 2020. doi: https://doi.org/10.1101/2020.05.01.072637.

29. Trager W, Jensen JB. Human malaria parasites in continuous culture. 1976. The Journal of parasitology. 2005;91(3):484-6. doi: 10.1645/0022-3395(2005)091[0484:HMPICC]2.0.CO;2. PubMed PMID: 16108535.

30. Lambros C, Vanderberg JP. Synchronization of Plasmodium falciparum erythrocytic stages in culture. The Journal of parasitology. 1979;65(3):418-20. PubMed PMID: 383936.

31. Sato S, Rangachari K, Wilson RJ. Targeting GFP to the malarial mitochondrion. Molecular and biochemical parasitology. 2003;130(2):155-8. PubMed PMID: 12946854.

32. Crabb BS, Rug M, Gilberger TW, Thompson JK, Triglia T, Maier AG, et al. Transfection of the human malaria parasite Plasmodium falciparum. Methods in molecular biology. 2004;270:263-76. doi: 10.1385/1-59259-793-9:263. PubMed PMID: 15153633.

33. Elsworth B, Matthews K, Nie CQ, Kalanon M, Charnaud SC, Sanders PR, et al. PTEX is an essential nexus for protein export in malaria parasites. Nature. 2014;511(7511):587-91. Epub 2014/07/22. doi: 10.1038/nature13555. PubMed PMID: 25043043.

34. Chugh M, Sundararaman V, Kumar S, Reddy VS, Siddiqui WA, Stuart KD, et al. Protein complex directs hemoglobin-to-hemozoin formation in Plasmodium falciparum. Proc Natl Acad Sci U S A. 2013;110(14):5392-7. Epub 2013/03/09. doi: 10.1073/pnas.1218412110. PubMed PMID: 23471987; PubMed Central PMCID: PMCPMC3619337.

Figures and Legends

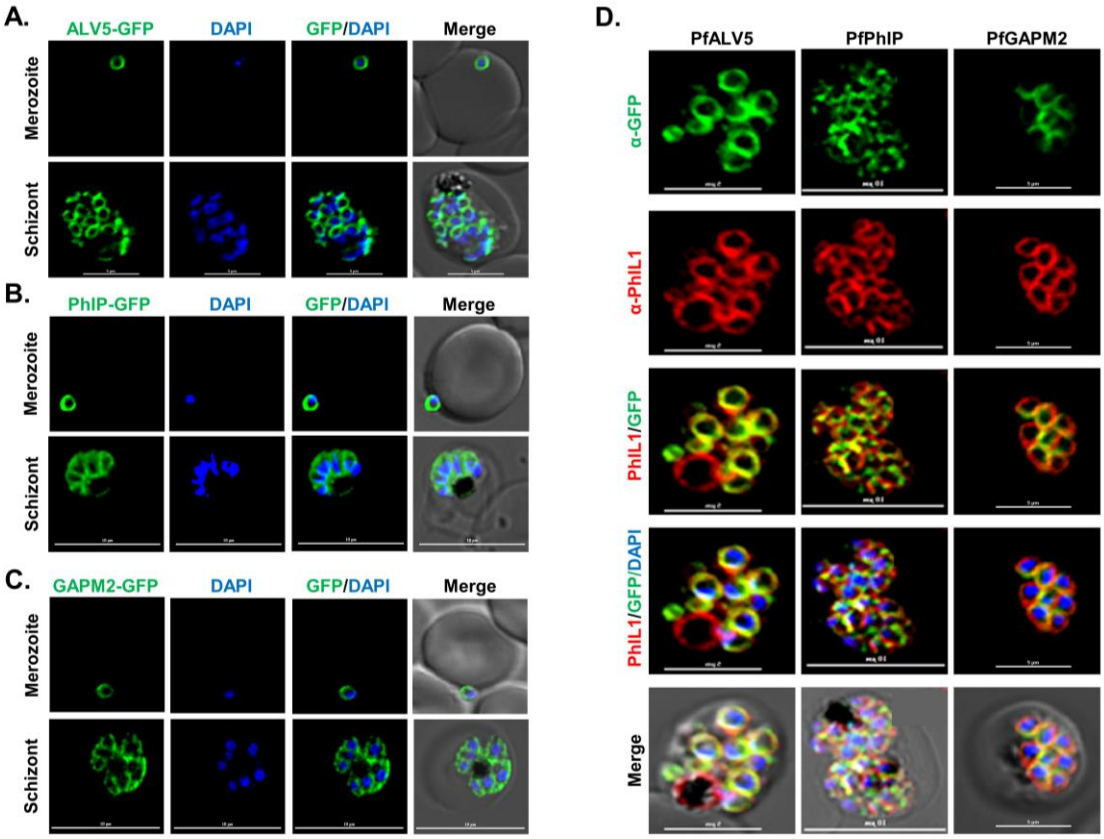

E.

Gene ID	Proteins pulled down by GFP-TRAP	No. of peptides		
		ALV5	PhIP	GAPM2
PF3D7_1003600	Membrane skeletal protein IMC1-related (ALV5)	12	4	3
PF3D7_0525800	Membrane skeletal protein IMC1-related	14	5	4
PF3D7_0918000	Secreted acid phosphatase (GAP50)	7	4	14
PF3D7_0822900	Conserved Plasmodium protein, unknown function	8	-	6
PF3D7_1310700	Conserved Plasmodium protein, unknown function	2	3	2
PF3D7_0109000	Photosensitized INA-labeled protein 1, PhIL1, putative	4	-	4
PF3D7_1406800	Glideosome associated protein with multiple membrane spans 3 (GAPM3)	4	-	5
PF3D7_0423500	Glideosome associated protein with multiple membrane spans 2 (GAPM2)	3	-	4
PF3D7_1323700	Glideosome associated protein with multiple membrane spans 1 (GAPM1)	1	-	-
PF3D7_1246400	Myosin light chain 1,myosin A tail domain interacting protein (MTIP)	1	-	-
PF3D7_1222700	Glideosome-associated protein 45 (GAP45)	1	-	1
PF3D7_0304000	Inner membrane complex protein 1a, putative (IMC1a)	1	-	-
PF3D7_0613900	Myosin E, putative (MyoE)	1	-	2
PF3D7_1342600	Myosin A (MyoA)	-	1	1

Fig 1: <u>PhIL1 co-exists with ALV5, PHIP, and GAPM2 in the *P. falciparum* IMC</u>: (A) ALV5-GFP expression pattern in asexual blood stages (merozoite, and schizont) of *P. falciparum*. **(B)** PhIP-GFP expression pattern in asexual blood stages showed typical IMC localisation. **(C)** GAPM2-GFP expression pattern in asexual blood stages. **(D)** Co-staining of PhIL1 with ALV5, PhIP and GAPM2 in *P. falciparum* blood-stage schizont. These proteins co-localised with PhIL1 in the IMC at schizont stage of the parasite with a Pearson's colocalization coefficient of more than 0.7. Scale bar = 5 μm. **(E)** List of proteins pulled down by GFP-Trap beads from lysates of ALV5, PhIP and GAPM2-GFP parasites, respectively. n = 3 experiments.

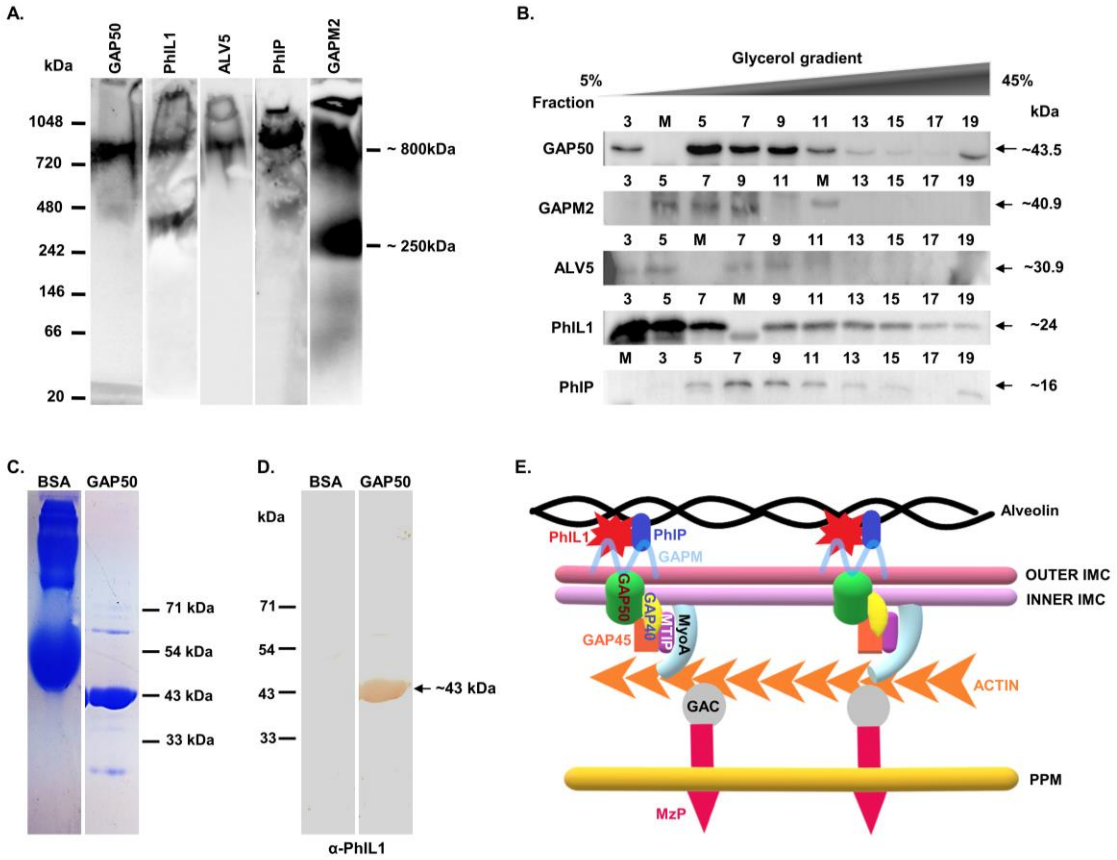

Fig 2: <u>PhIL1 associated novel complex overlaps with components of the linear motor in the IMC but is a separate complex</u>: (A) Native PAGE analysis of schizont stage parasite lysate shows co-existence of PhIL1 associated complex with the glideosomal complex via. some overlapping components. A complex of ~800 kDa was detected containing components of PfPhIL1 associated complex and GAP50. Furthermore, a smaller complex of ~250 kDa was also detected that included PfPhIL1 and PfGAPM2. These results indicate a possible association of PhIL1 associated complex and glideosomal complex. n = 2 experiments. **(B)** PhIL1 associated complex co-exists with the glideosomal complex as seen by Glycerol gradient co-sedimentation analysis. Glycerol gradient fractionation of *P. falciparum* schizont extract using 5 to 45% Glycerol gradient followed by immunoblotting of the fractions using specific antibodies showed the co-sedimentation of PfGAP50, PfPhIL1, PfALV5, PfPhIP and PfGAPM2 together in fractions 5 to 11, particularly, in fraction 9 corresponding to ~250 kDa molecular mass. n = 2 experiments. **(C)** Recombinant GAP50 and BSA were subjected to SDS-PAGE followed by **(D)** Far western analysis showing interaction of recombinant PfGAP50 protein with PfPhIL1. GAP50 was denatured and renatured on the membrane followed by incubation with recombinant PhIL1 protein and probed with α-PhIL1 antisera, which recognised a band of ~43kDa corresponding to the size of GAP50. BSA used as control protein did not show any interaction with PfPhIL1. **(E)** Prototype showing molecular motor and partially overlying proposed PhIL1 associated complex in the parasite IMC. Photosensitized 5-[^{125}I] Iodonaphthalene-1-azide Labelled Protein-1 (PhIL1); **Ph**IL1 **I**nteracting **P**rotein (PhIP); Glideosome-associated protein 40, 45 and 50 (GAP40, 45 and 50); Glideosome-associated protein with multiple membrane spans (GAPM); myosin-A (MyoA); myosin-A tail domain interacting protein (MTIP); Glideosome Associated Connector (GAC); Protein of the Merozoite surface (MzP); Parasite Plasma Membrane (PPM).

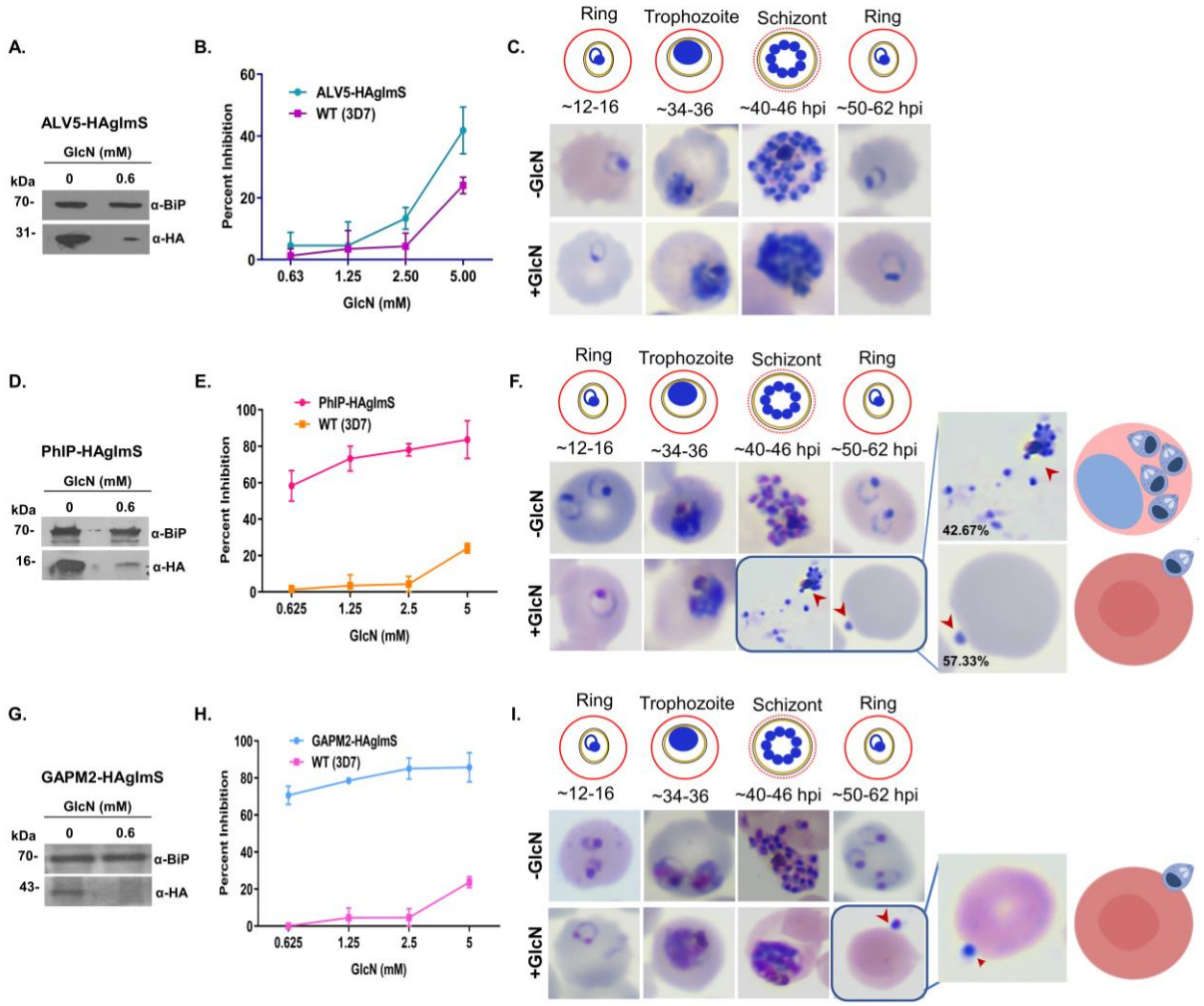

Fig 3: <u>Functional characterization of *P. falciparum* ALV5, PhIP and GAPM2 by inducible regulation of endogenous protein levels and their effect on parasite growth</u>: **(A)** Western blot analysis of lysate from PfALV5-pHA-*glmS* line with α-HA rat serum showing conditional knock-down on glucosamine treatment. **(B)** Effect of conditional knockdown of PfALV5 on parasite invasion of the host RBC. Glucosamine-treated (+GlcN) and untreated (-GlcN) cultures were incubated till the formation of new rings and the parasitaemia was estimated by flow cytometry. **(C)** Representative parasites from the Giemsa-stained smears showing morphology following ALV5 knockdown. **(D)** Western blot analysis of lysate from PfPhIP-HA-*glmS* line with α-HA rat antibody to check for conditional knock-down shows a robust knockdown of PhIP-HA protein. **(E)** Effect of conditional knockdown of PfPhIP on parasite invasion. **(F)** Representative parasites from the Giemsa-stained smears showing morphology following PhIP knockdown. Percentage of different phenotypes was calculated from Giemsa smears of glucosamine treated PhIP-HA-*glmS* parasites, highlighting the arrest of growth in segmented schizont stage, and altered efficacy of released merozoites to invade following PhIP knockdown. See also Fig S4. **(G)** Western blot analysis of lysate from PfGAPM2-HA-*glmS* line with α-HA rat serum showing efficient knockdown of the GAPM2-HA protein when compared to the anti-*Pf*BiP loading control. **(H)** Effect of conditional knockdown of PfGAPM2 in parasite showing up to 85% invasion inhibition. **(I)** Representative Giemsa-stained smears showing the arrest in development following GAPM2 knockdown due to inefficiency of released merozoites to invade the host RBC. Zoomed Giemsa smear show phenotype for PhIP- and GAPM2-HA-*glmS* parasites plus glucosamine, highlighting the arrest in development following knockdown. Data represents mean ± SD. n = 3 experiments. Anti-*Pf*BiP was used as loading control for western blot analysis.

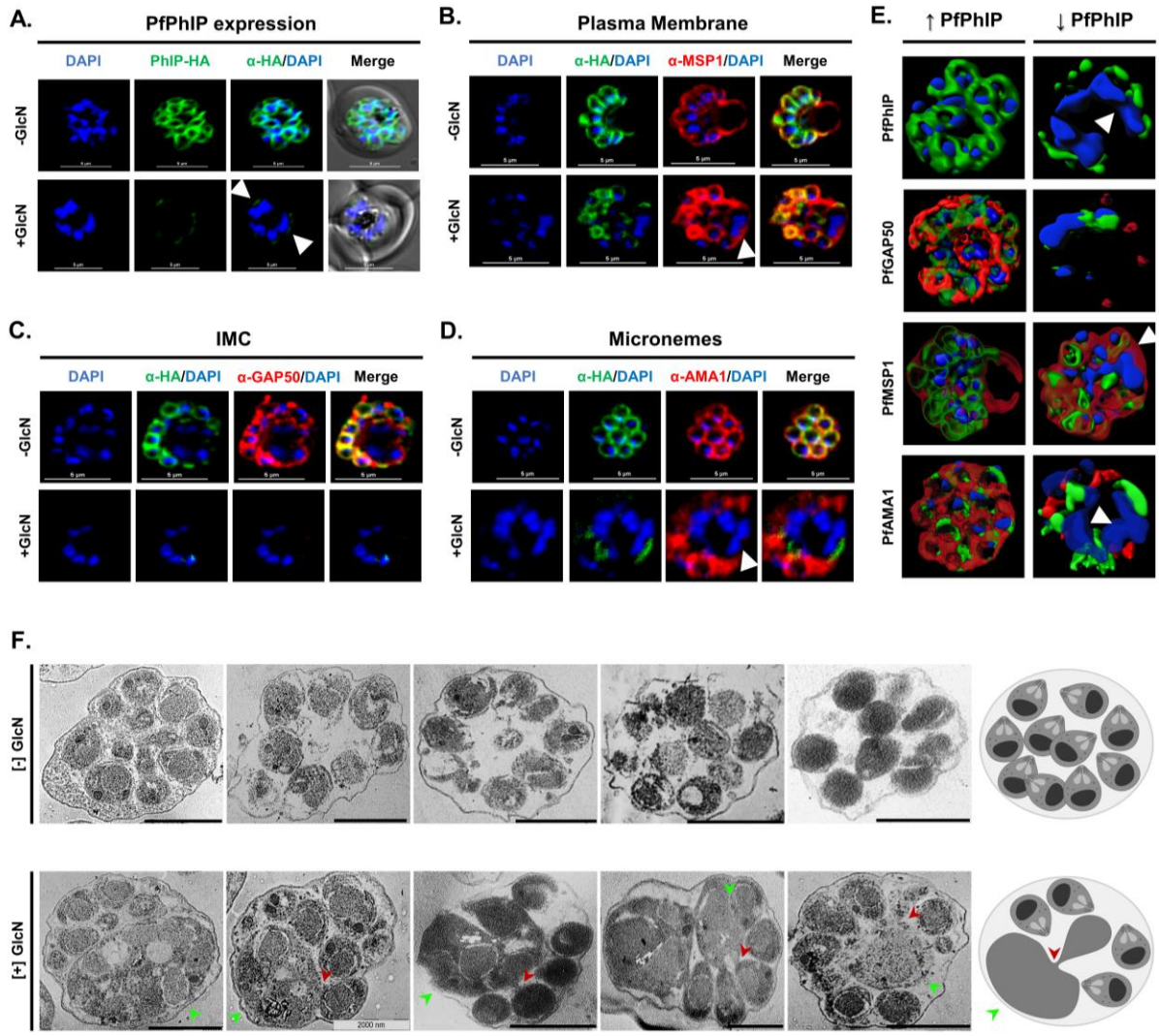

Fig 4: <u>PfPhIP deficient parasites show defects in segmentation of daughter cells</u>: PfPhIP-HA-*glmS* parasites maintained with and without GlcN were E64-treated (10 µM) and probed with the anti-HA antibody (green) and counterstained with DAPI. **(A)** Apparent knockdown of PhIP expression leads to formation of agglomerates of unsegmented daughter nuclei. **(B)** Anti-GAP50 antibody (IMC marker) (red) showed defects in IMC formation in agglomerates. Merozoite plasma membrane and micronemes were stained with antibodies against *P. falciparum* **(C)** merozoite surface protein 1 (PfMSP1) (red) and **(D)** PfAMA1 (red), respectively, in E64-treated schizonts cultivated with and without GlcN. PfMSP1 was visible in schizonts but forms relatively larger rings that surround multiple nuclei in the agglomerates. PfAMA1 showed loss of signal in agglomerates. Scale bar = 5 µm. **(E)** 3D reconstruction of the PfPhIP-HA-*glmS* schizonts with and without GlcN is presented using Imaris 7.6.1. Arrowheads indicate agglomerates of unsegmented daughter nuclei. See also Fig S5. **(F)** Transmission electron micrographs of PfPhIP-HAglmS parasites [-] and [+] GlcN. Arrowheads in PfPhIP-deficient schizonts point to incompletely segmented daughter cells (red) and agglomerates of multiple daughter nuclei (green), while distinct membrane enclosed merozoites with well-arranged apical organelles were observed in GlcN untreated schizonts. Scale bars = 2000 nm.

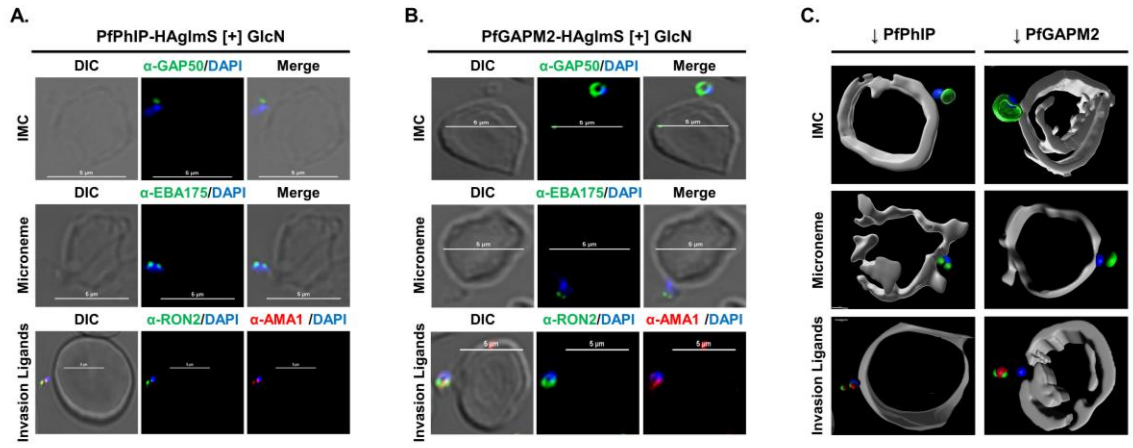

Fig 5: <u>PfGAPM2 and PfPhIP function is essential for invasion of the host cell by the merozoites</u>: Merozoites released from GlcN treated **(A)** PfPhIP-HA-glmS and **(B)** PfGAPM2-HA-glmS parasites were stained using antibodies against PfGAP50 (green, top panel), PfEBA175 (green, middle panel), PfRON2 (green) and PfAMA1 (red) (lower panel). Staining for these markers showed normal micronemal and rhoptry organelles, however, it was observed that the discharge of contents from these apical organelles was affected. Also, the apical end of the merozoites, attached to the host was not aligned towards the erythrocyte membrane. Scale bar = 5 µm. **(C)** 3D reconstruction of the merozoites from PfPhIP or PfGAPM2 deficient parasites arrested on the RBC surface using Imaris 9. See also Fig S6.

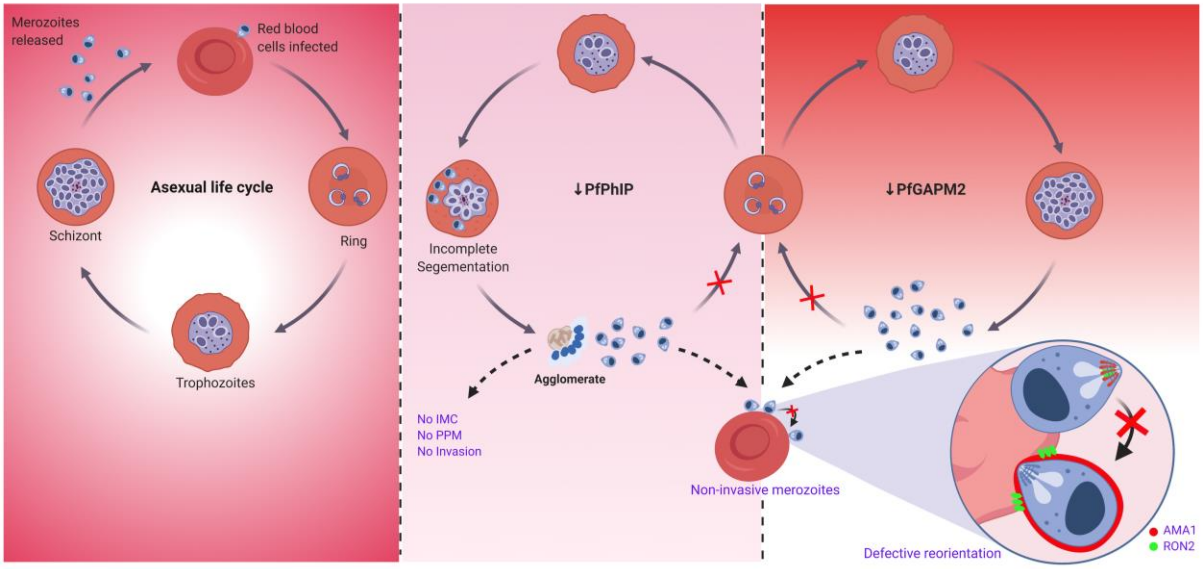

Fig 6: <u>Function of PhIL1 associated complex is crucial for reorientation mediated by gliding motor complex and thus host-cell invasion by *Plasmodium falciparum* merozoites</u>: The schematic illustrates GAPM2 and PhIP are essential for blood stage infection and their genetic attenuation arrests merozoite invasion by impeding the function of glideosomal motor machinery resulting in failure of merozoite to reorient its apical end towards the host RBC. Depletion of PhIP also leads to formation of agglomerates of unsegmented schizonts suggesting its probable role in IMC mediated parasite cell division. In the left panel, the level of PfPhIP or GAPM2 protein is maintained by the absence of GlcN. Middle panel shows consequences of PhIP deficiency, wherein a portion of daughter cells get segmented while others remain trapped as an agglomerate under a common plasma membrane. In the agglomerate, IMC fails to form, parasite plasma membrane surrounds multinucleated unsegmented daughter cell, and microneme secretion is affected. Few segmented merozoites which egressed, were seen arrested at the erythrocyte surface and are unable to invade. Right panel summarises the effect of GAPM2 deficiency in the parasite where the merozoites fail to invade the erythrocytes due to the disability of these merozoites to align their apical end towards the host cell surface. Apical reorientation of merozoites is imperative for invasion so that the apical organelles are aligned to the erythrocyte membrane which leads to discharge of apical organellar proteins followed by invasion. Created with BioRender.com

Supplemental Figures and Legends

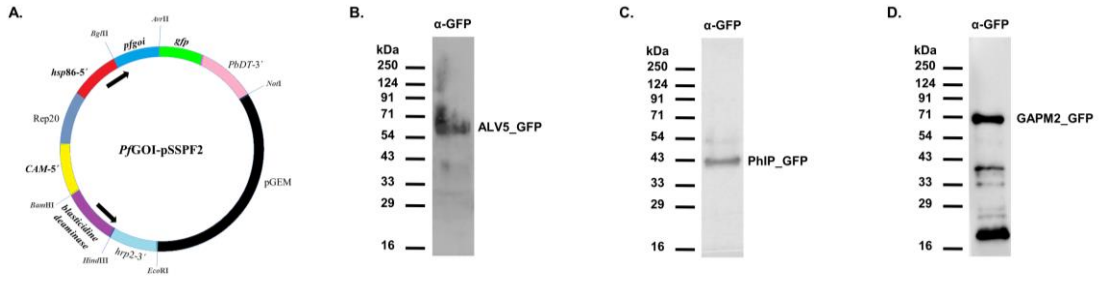

Fig S1: <u>Generation and conformation of PfALV5-, PfPhIP- and PfGAPM2-GFP fusion parasite lines</u>: (A) Schematic showing vector map of pSSPF2 construct, indicating different vector cassettes used for generation of GFP protein in fusion with PfALV5, PfPhIP or PfGAPM2. Western blot analysis of lysate from **(B)** PfALV5-GFP, **(C)** PfPhIP-GFP, and **(D)** PfGAPM2-GFP tag line, with α-GFP rabbit serum. M denotes known molecular weight marker.

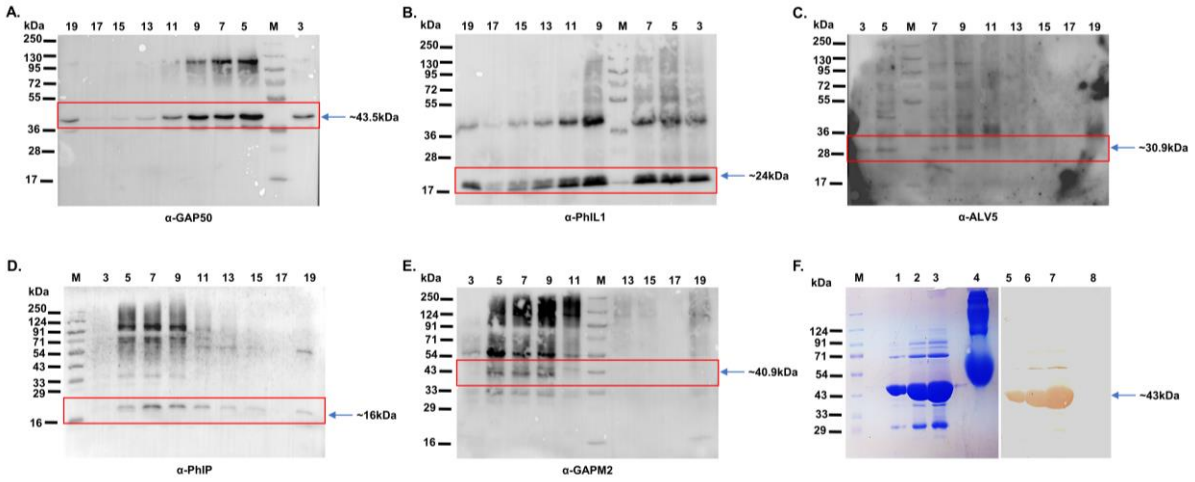

Fig S2: <u>Glycerol gradient fractionation for cosedimentation of PhIL1 associated complex along with PfGAP50</u>: Western blot analysis following glycerol gradient centrifugation in *P. falciparum* blood-stage schizonts using protein specific antibodies for: **(A)** PfGAP50 **(B)** PfPhIL1 **(C)** PfALV5 **(D)** PfPhIP and **(E)** PfGAPM2. n = 2 experiments. **(F)** Protein-protein interaction between PfPhIL1 and PfGAP50 was further confirmed using Far western blotting. Recombinant GAP50 protein was subjected to SDS-PAGE (lane 1, 2 and 3 having 0.7, 2.8 and 7 µg of purified protein respectively) and transferred to PVDF membrane. Proteins were denatured on the membrane followed by renaturation and subsequently incubated with 14 µg rPhIL1 protein. Blot was probed with α-PhIL1 antibody (lane 5, 6, 7, and 8). BSA (lane 4 and 8; 10 µg) was used as a control. M denotes known molecular weight marker.

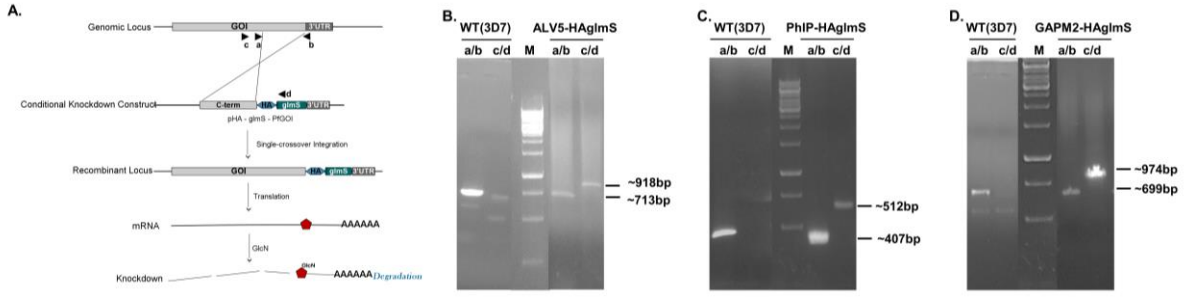

Fig S3: <u>Generation of PfALV5, PfPhIP and PfGAPM2 inducible knockdown parasite lines</u>: (A) Schematic of the *glmS* ribozyme reverse genetic tool: The ribozyme is inserted in the 3′-UTR after the coding region so that it is present in the expressed mRNA. Following addition of the inducer, glucosamine, which binds to the ribozyme, the mRNA self-cleaves resulting in degradation of the mRNA and knock down of protein expression. Integration into the parasite genome was confirmed by PCR using different primer sets: cloned C-terminus region (a/b), upstream of cloned region (c) and from the *glm*S ribozyme sequence, 1236A (d). Position of primers are marked by arrowheads. **(B)** PfALV5-pHA_*glmS* integrants in parasite genome were selected by PCR analysis using primer sets: 1003600_$F_{glmS\text{-}HA}$ (a) / 1003600_$R_{glmS\text{-}HA}$ (b) and 1003600_Int. (c) /1236A (d). **(C)** PCR was set up for confirmation of successful integration of PfPhIP-pHA_*glmS* construct in parasite genome using different set of primers: 1310700_$F_{glmS\text{-}HA}$ (a) /1310700_$R_{glmS\text{-}HA}$ (b) and 1310700_Int (c) /1236A (d). **(D)** Successful integration of PfGAPM2-pHA_*glmS* construct in parasite genome was confirmed using primer set: 0423500_$F_{glmS\text{-}HA}$ (a) / 0423500_$R_{glmS\text{-}HA}$ (b) and 0423500_Int. (c) / 1236A (d). M denotes known molecular weight marker.

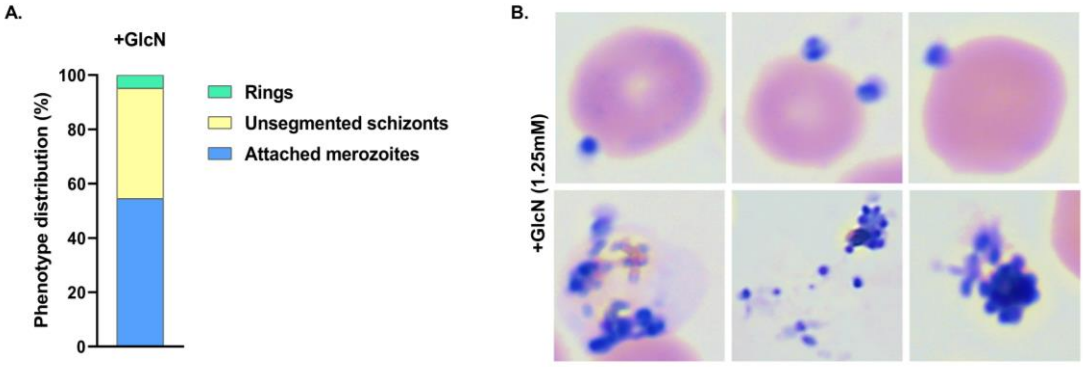

Fig S4: <u>The two distinct phenotypes observed in PhIP knock-down parasites demonstrate the divergent functions of the components of IMC during asexual lifecycle of the parasite</u>. (A) Number of parasites showing the arrest in development following knockdown due to two different phenotypes was calculated from Giemsa-stained smears of PhIP-HA-*glmS* parasites after 42 h of glucosamine treatment (1.25 mM). **(B)** Representative parasites from the Giemsa-stained smears showing agglomerates and arrested merozoites following PfPhIP knockdown.

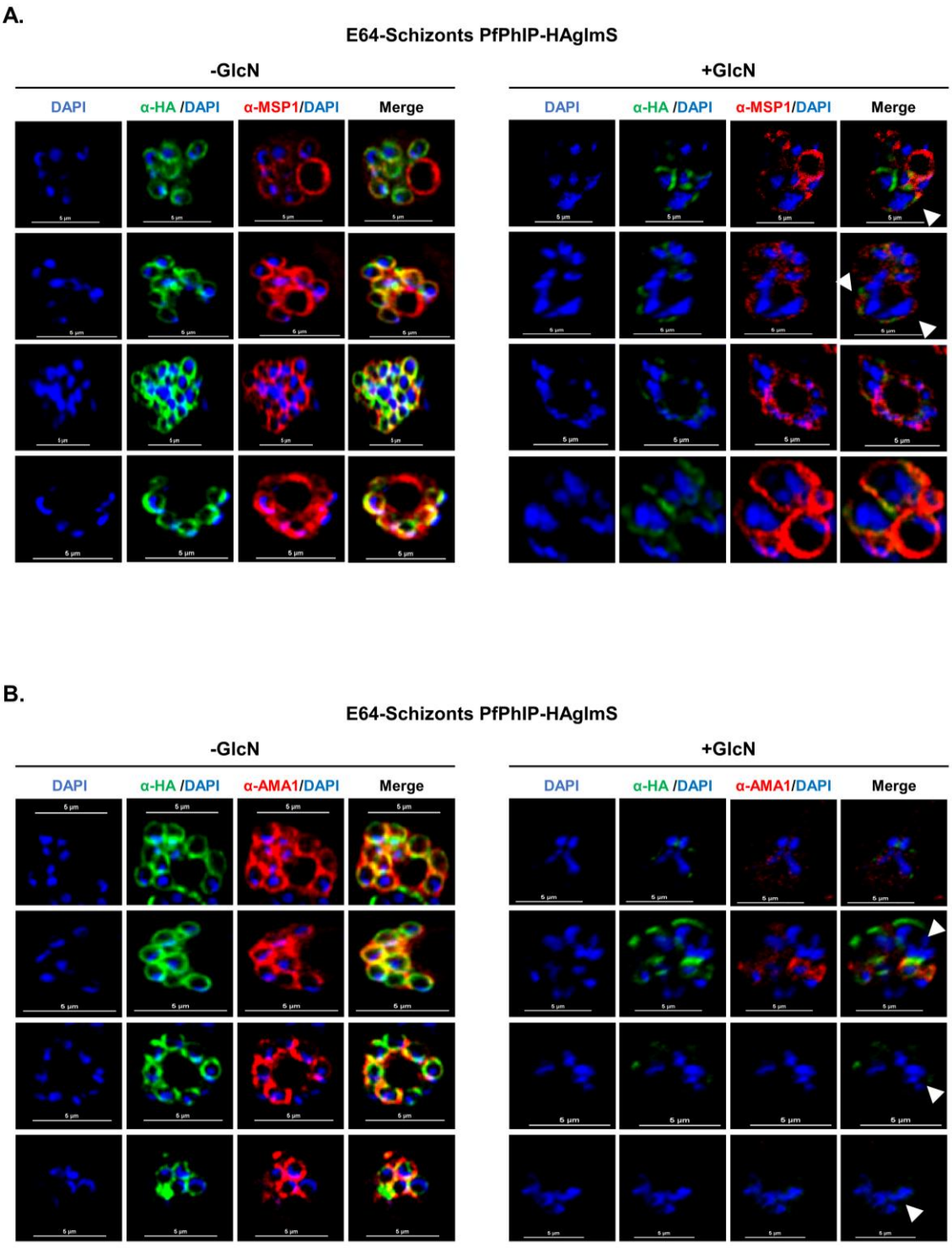

Fig S5: <u>PfPhIP deficiency leads to incomplete formation of the IMC</u>. Representative images of E64-treated schizont stage in [-]/ [+] GlcN PfPhIP-HA-*glmS* parasites using antibodies against **(A)** PfMSP1 and **(B)** PfAMA1. Arrowheads show agglomerates showing loss of signal for AMA1 and MSP1 in unsegmented nuclei. Scale bar = 5 µm.

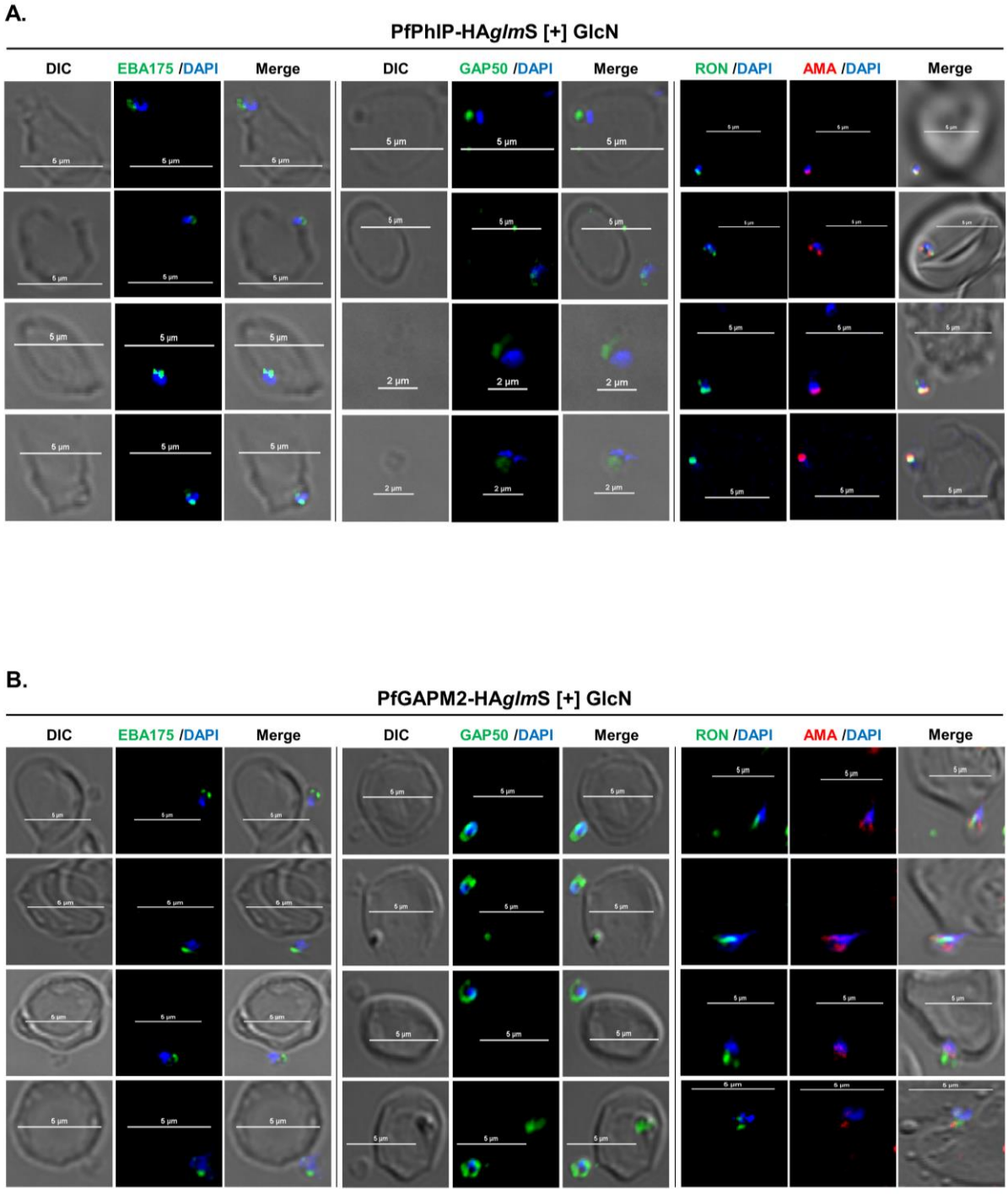

Fig S6: <u>Released merozoites from PfPhIP- and PfGAPM2-deficient schizonts fail to invade erythrocytes</u>. Merozoites appeared to be arrested at RBC surface due to failure to align its apical end towards the host cell were probed with DAPI; anti-RON2 (green), anti-GAP50 (green), anti-EBA175 antibody (green) and anti-AMA1 antibody (red) in **(A)** PfPhIP deficient merozoites **(B)** PfGAPM2 deficient merozoites. Scale bar = 5 µm.

Oligonucleotides used in this study

Name	Sequence 5' to 3'	Notes
Primers used for GFP tag construct		
1310700_F_{pSSPF2}	gcggtaccAGATCTGAAAAAATGGCTTTTTCACC	BglII restriction site AvrII restriction site
1310700_R_{pSSPF2}	gcCCTAGGATATTCCTCTTCTTCTTCTTCT	
0423500_F_{pSSPF2}	gcggtaccAGATCTATGGGTTCATACGGAATGG	
0423500_R_{pSSPF2}	gcCCTAGGATATTGAGCTGTCTTAATATAATTA	
1003600_F_{pSSPF2}	gcggtaccAGATCTGAAAAGTATAAAATGGCAG	
1003600_R_{pSSPF2}	gcCCTAGGAGTGCAGGCAGCTGAGC	
Primers used for Knockdown construct		
1310700_$F_{glmS\text{-}HA}$	gcAGATCTGAGTTAATTGTACCTCAAGACC	BglII restriction site PstI restriction site
1310700_$R_{glmS\text{-}HA}$	gcCTGCAGcATATTCCTCTTCTTCTTCTTC	
0423500_$F_{glmS\text{-}HA}$	gcAGATCTgtgattgcctgtacaaagtca	
0423500_$R_{glmS\text{-}HA}$	gcCTGCAGcATATTGAGCTGTCTTAATATAAT	
1003600_$F_{glmS\text{-}HA}$	gcAGATCTCCGTTGAAGTTCCAATTATTAAG	
1003600_$R_{glmS\text{-}HA}$	gcCTGCAGcAGTGCAGGCAGCTGAGC	
Primers used for confirmation of integration		
1310700_Int.	GAAAAAATGGCTTTTTCAC	Forward primer upstream of cloned C-term region of the gene
0423500_Int.	CCCTCTTCAAATTGGC	
1003600_Int.	GTATAAAATGGCAGATTC	
1236A	TACGGATACGCATAATCGG	Reverse primer +77bp downstream of PstI

Table S1: Oligonucleotides used in this study.

Figures

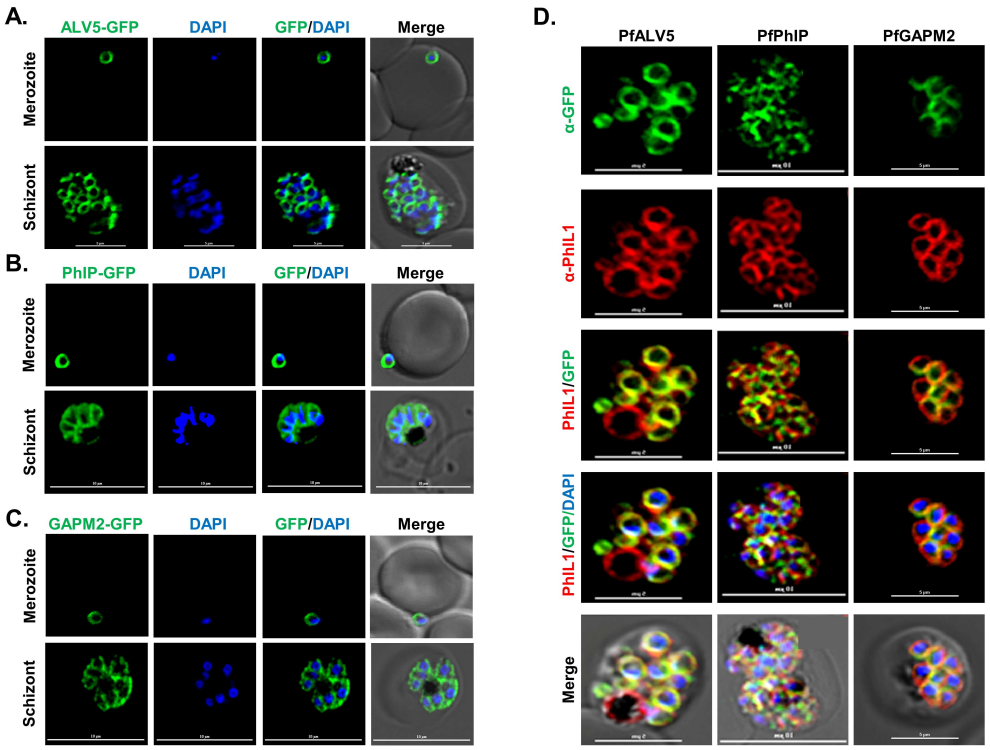

E.

Gene ID	Proteins pulled down by GFP-TRAP	No. of peptides		
		ALV5	PhIP	GAPM2
PF3D7_1003600	Membrane skeletal protein IMC1-related (ALV5)	12	4	3
PF3D7_0525800	Membrane skeletal protein IMC1-related	14	5	4
PF3D7_0918000	Secreted acid phosphatase (GAP50)	7	4	14
PF3D7_0822900	Conserved Plasmodium protein, unknown function	8	-	6
PF3D7_1310700	Conserved Plasmodium protein, unknown function	2	3	2
PF3D7_0109000	Photosensitized INA-labeled protein 1, PhIL1, putative	4	-	4
PF3D7_1406800	Glideosome associated protein with multiple membrane spans 3 (GAPM3)	4	-	5
PF3D7_0423500	Glideosome associated protein with multiple membrane spans 2 (GAPM2)	3	-	4
PF3D7_1323700	Glideosome associated protein with multiple membrane spans 1 (GAPM1)	1	-	-
PF3D7_1246400	Myosin light chain 1,myosin A tail domain interacting protein (MTIP)	1	-	-
PF3D7_1222700	Glideosome-associated protein 45 (GAP45)	1	-	1
PF3D7_0304000	Inner membrane complex protein 1a, putative (IMC1a)	1	-	-
PF3D7_0613900	Myosin E, putative (MyoE)	1	-	2
PF3D7_1342600	Myosin A (MyoA)	-	1	1

Figure 1

PhIL1 co-exists with ALV5, PHIP, and GAPM2 in the P. falciparum IMC: (A) ALV5-GFP expression pattern in asexual blood stages (merozoite, and schizont) of P. falciparum. (B) PhIP-GFP expression pattern in asexual blood stages showed typical IMC localisation. (C) GAPM2-GFP expression pattern in asexual

blood stages. (D) Co-staining of PhIL1 with ALV5, PhIP and GAPM2 in P. falciparum blood-stage schizont. These proteins co-localised with PhIL1 in the IMC at schizont stage of the parasite with a Pearson's colocalization coefficient of more than 0.7. Scale bar = 5 µm. (E) List of proteins pulled down by GFP-Trap beads from lysates of ALV5, PhIP and GAPM2-GFP parasites, respectively. n = 3 experiments.

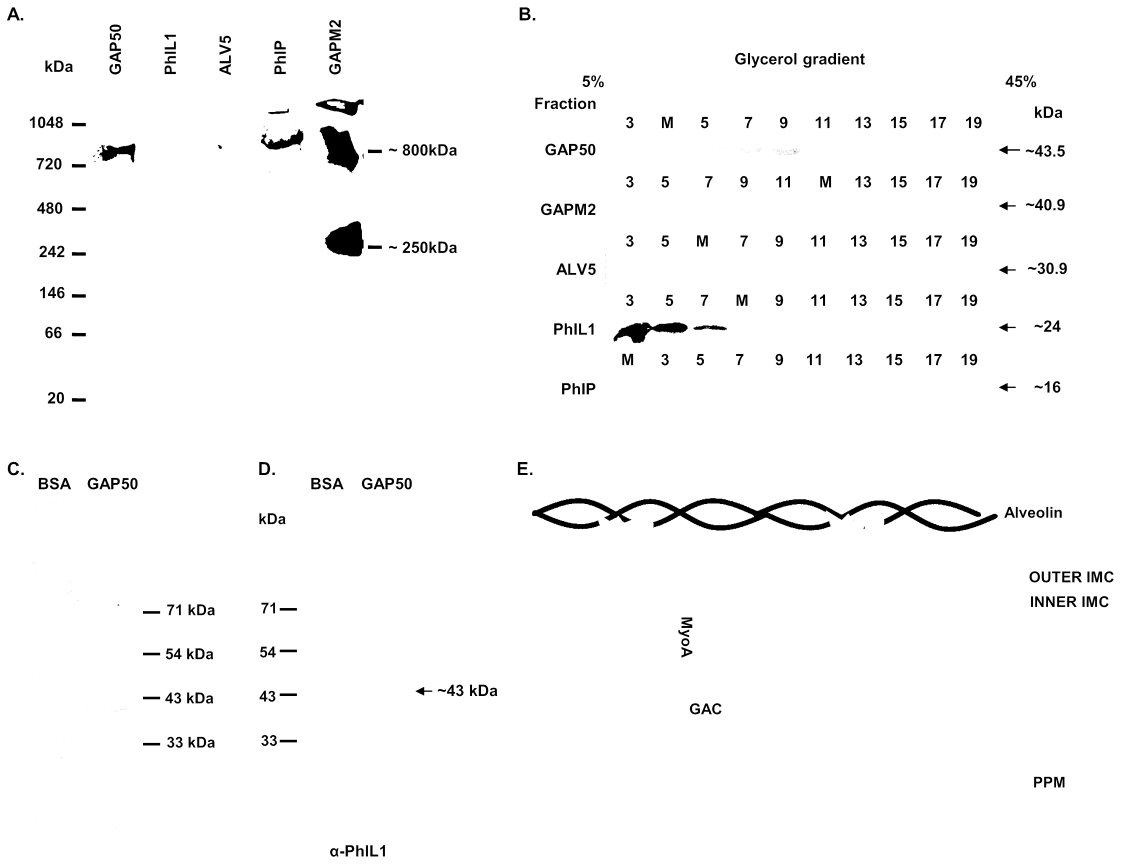

Figure 2

PhIL1 associated novel complex overlaps with components of the linear motor in the IMC but is a separate complex: (A) Native PAGE analysis of schizont stage parasite lysate shows co-existence of PhIL1 associated complex with the glideosomal complex via. some overlapping components. A complex of ~800 kDa was detected containing components of PfPhIL1 associated complex and GAP50. Furthermore, a smaller complex of ~250 kDa was also detected that included PfPhIL1 and PfGAPM2. These results indicate a possible association of PhIL1 associated complex and glideosomal complex. n = 2 experiments. (B) PhIL1 associated complex co-exists with the glideosomal complex as seen by Glycerol gradient co-sedimentation analysis. Glycerol gradient fractionation of P. falciparum schizont extract using 5 to 45% Glycerol gradient followed by immunoblotting of the fractions using specific antibodies showed the co-sedimentation of PfGAP50, PfPhIL1, PfALV5, PfPhIP and PfGAPM2 together in fractions 5 to 11, particularly, in fraction 9 corresponding to ~250 kDa molecular mass. n = 2 experiments. (C) Recombinant GAP50 and BSA were subjected to SDS-PAGE followed by (D) Far western analysis showing interaction of recombinant PfGAP50 protein with PfPhIL1. GAP50 was denatured and renatured on the membrane followed by incubation with recombinant PhIL1 protein and probed with α-PhIL1 antisera, which recognised a band of ~43kDa corresponding to the size of GAP50. BSA used as control protein did not show any interaction with PfPhIL1. (E) Prototype showing molecular motor and partially overlying proposed PhIL1 associated complex in the parasite IMC. Photosensitized 5-[125I] Iodonaphthalene-1-azide Labelled Protein-1 (PhIL1); PhIL1 Interacting Protein (PhIP); Glideosome-associated protein 40, 45 and 50 (GAP40, 45 and 50); Glideosome-associated protein with multiple membrane spans (GAPM); myosin-A (MyoA); myosin-A tail domain interacting protein (MTIP); Glideosome Associated Connector (GAC); Protein of the Merozoite surface (MzP); Parasite Plasma Membrane (PPM).

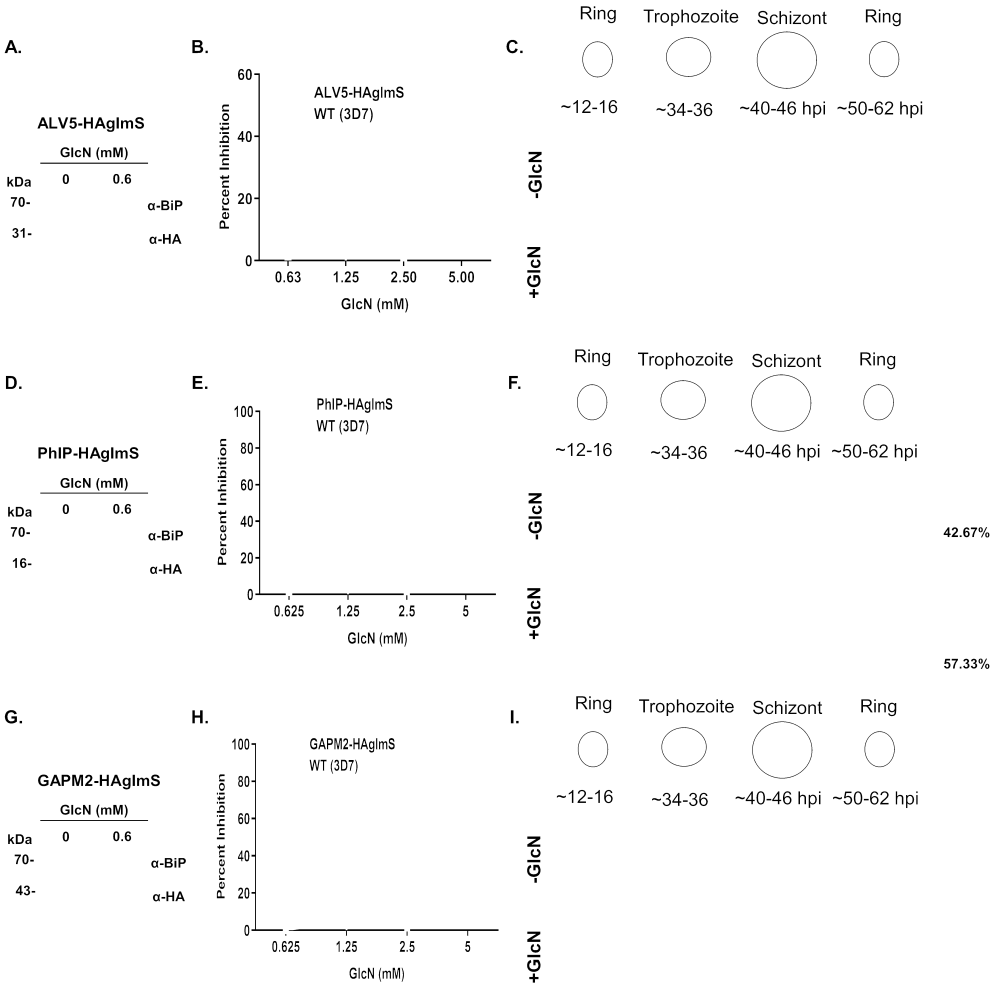

Figure 3

Functional characterization of P. falciparum ALV5, PhIP and GAPM2 by inducible regulation of endogenous protein levels and their effect on parasite growth: (A) Western blot analysis of lysate from PfALV5-pHA-glmS line with α-HA rat serum showing conditional knock-down on glucosamine treatment. (B) Effect of conditional knockdown of PfALV5 on parasite invasion of the host RBC. Glucosamine-treated (+GlcN) and untreated (-GlcN) cultures were incubated till the formation of new rings and the

parasitaemia was estimated by flow cytometry. (C) Representative parasites from the Giemsa-stained smears showing morphology following ALV5 knockdown. (D) Western blot analysis of lysate from PfPhIP-HA-glmS line with α-HA rat antibody to check for conditional knock-down shows a robust knockdown of PhIP-HA protein. (E) Effect of conditional knockdown of PfPhIP on parasite invasion. (F) Representative parasites from the Giemsa-stained smears showing morphology following PhIP knockdown. Percentage of different phenotypes was calculated from Giemsa smears of glucosamine treated PhIP-HA-glmS parasites, highlighting the arrest of growth in segmented schizont stage, and altered efficacy of released merozoites to invade following PhIP knockdown. See also Fig S4. (G) Western blot analysis of lysate from PfGAPM2-HA-glmS line with α-HA rat serum showing efficient knockdown of the GAPM2-HA protein when compared to the anti-PfBiP loading control. (H) Effect of conditional knockdown of PfGAPM2 in parasite showing up to 85% invasion inhibition. (I) Representative Giemsa-stained smears showing the arrest in development following GAPM2 knockdown due to inefficiency of released merozoites to invade the host RBC. Zoomed Giemsa smear show phenotype for PhIP- and GAPM2-HA-glmS parasites plus glucosamine, highlighting the arrest in development following knockdown. Data represents mean ± SD. n = 3 experiments. Anti-PfBiP was used as loading control for western blot analysis.

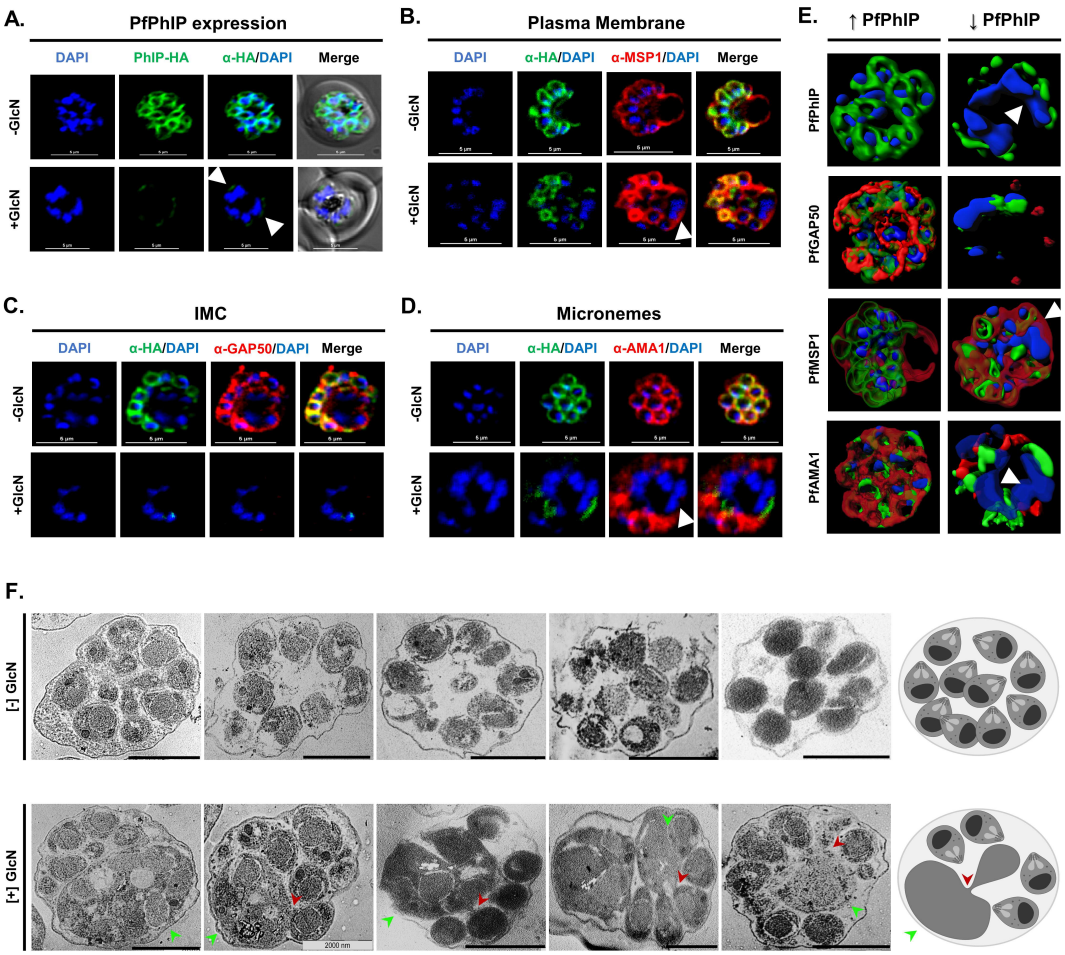

Figure 4

PfPhIP deficient parasites show defects in segmentation of daughter cells: PfPhIP-HA-glmS parasites maintained with and without GlcN were E64-treated (10 μM) and probed with the anti-HA antibody (green) and counterstained with DAPI. (A) Apparent knockdown of PhIP expression leads to formation of agglomerates of unsegmented daughter nuclei. (B) Anti-GAP50 antibody (IMC marker) (red) showed defects in IMC formation in agglomerates. Merozoite plasma membrane and micronemes were stained

with antibodies against P. falciparum (C) merozoite surface protein 1 (PfMSP1) (red) and (D) PfAMA1 (red), respectively, in E64-treated schizonts cultivated with and without GlcN. PfMSP1 was visible in schizonts but forms relatively larger rings that surround multiple nuclei in the agglomerates. PfAMA1 showed loss of signal in agglomerates. Scale bar = 5 μm. (E) 3D reconstruction of the PfPhIP-HA-glmS schizonts with and without GlcN is presented using Imaris 7.6.1. Arrowheads indicate agglomerates of unsegmented daughter nuclei. See also Fig S5. (F) Transmission electron micrographs of PfPhIP-HAglmS parasites [-] and [+] GlcN. Arrowheads in PfPhIP-deficient schizonts point to incompletely segmented daughter cells (red) and agglomerates of multiple daughter nuclei (green), while distinct membrane enclosed merozoites with well-arranged apical organelles were observed in GlcN untreated schizonts. Scale bars = 2000 nm.

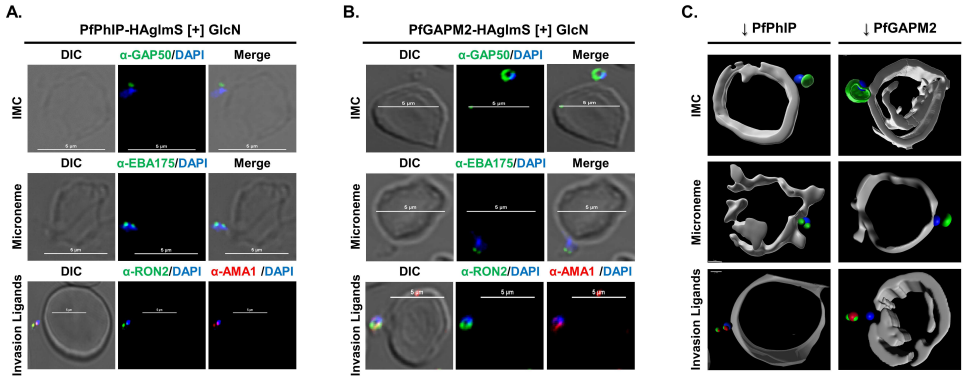

Figure 5

PfGAPM2 and PfPhIP function is essential for invasion of the host cell by the merozoites: Merozoites released from GlcN treated (A) PfPhIP-HA-glmS and (B) PfGAPM2-HA-glmS parasites were stained using antibodies against PfGAP50 (green, top panel), PfEBA175 (green, middle panel), PfRON2 (green) and PfAMA1 (red) (lower panel). Staining for these markers showed normal micronemal and rhoptry organelles, however, it was observed that the discharge of contents from these apical organelles was affected. Also, the apical end of the merozoites, attached to the host was not aligned towards the erythrocyte membrane. Scale bar = 5 μm. (C) 3D reconstruction of the merozoites from PfPhIP or PfGAPM2 deficient parasites arrested on the RBC surface using Imaris 9. See also Fig S6.

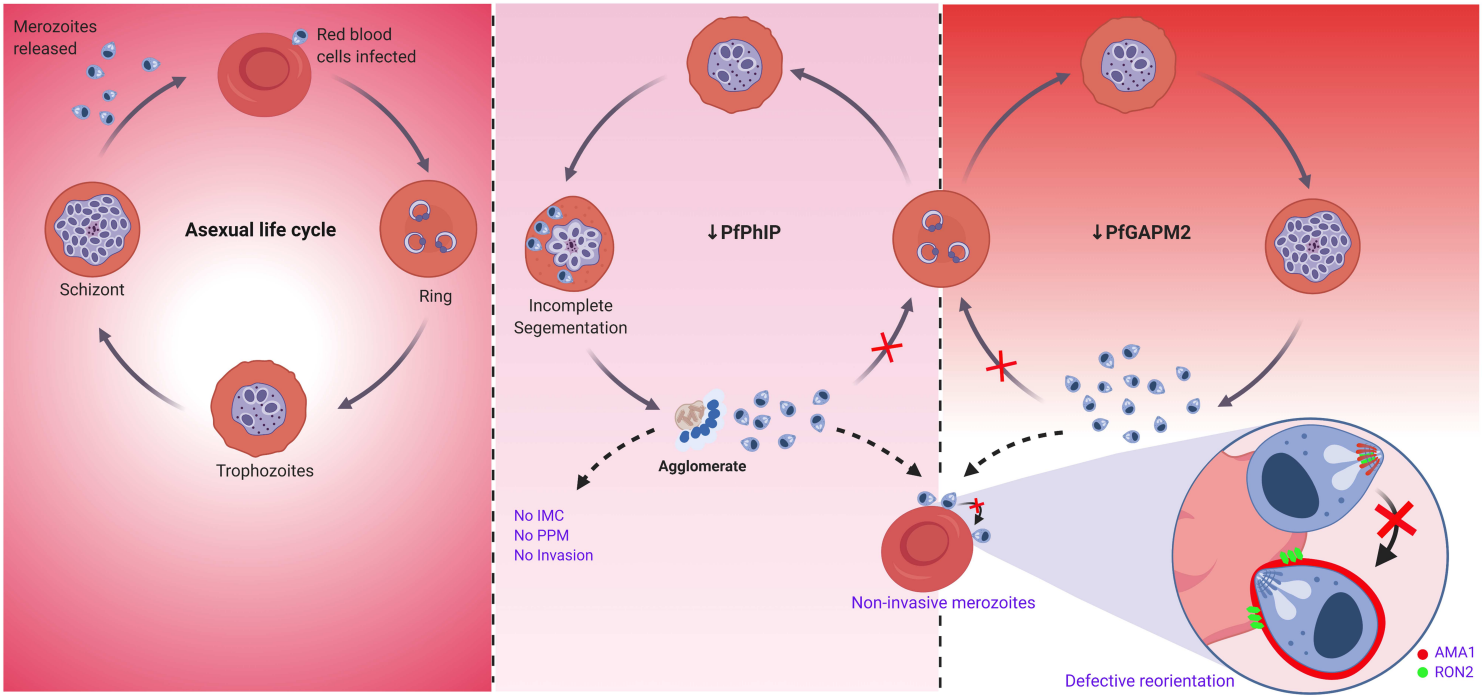

Figure 6

Function of PhIL1 associated complex is crucial for reorientation mediated by gliding motor complex and thus host-cell invasion by Plasmodium falciparum merozoites: The schematic illustrates GAPM2 and PhIP are essential for blood stage infection and their genetic attenuation arrests merozoite invasion by impeding the function of glideosomal motor machinery resulting in failure of merozoite to reorient its apical end towards the host RBC. Depletion of PhIP also leads to formation of agglomerates of unsegmented schizonts suggesting its probable role in IMC mediated parasite cell division. In the left panel, the level of PfPhIP or GAPM2 protein is maintained by the absence of GlcN. Middle panel shows consequences of PhIP deficiency, wherein a portion of daughter cells get segmented while others remain trapped as an agglomerate under a common plasma membrane. In the agglomerate, IMC fails to form, parasite plasma membrane surrounds multinucleated unsegmented daughter cell, and microneme secretion is affected. Few segmented merozoites which egressed, were seen arrested at the erythrocyte surface and are unable to invade. Right panel summarises the effect of GAPM2 deficiency in the parasite where the merozoites fail to invade the erythrocytes due to the disability of these merozoites to align their apical end towards the host cell surface. Apical reorientation of merozoites is imperative for invasion so that the apical organelles are aligned to the erythrocyte membrane which leads to discharge of apical organellar proteins followed by invasion. Created with BioRender.com

Supplementary Files

This is a list of supplementary files associated with this preprint. Click to download.

- FigS1.tif
- FigS2.tif
- FigS3.tif
- FigS4.tif
- FigS5.tif
- FigS6.tif
- FigS7.tif